

# 1 Evaluating the dendroclimatological potential of blue intensity on 2 multiple conifer species from Tasmania and New Zealand

3 Rob Wilson<sup>1,4</sup>, Kathy Allen<sup>2</sup>, Patrick Baker<sup>2</sup>, Gretel Boswijk<sup>3</sup>, Brendan Buckley<sup>4</sup>, Edward Cook<sup>4</sup>,  
4 Rosanne D'Arrigo<sup>4</sup>, Dan Druckenbrod<sup>5</sup>, Anthony Fowler<sup>3</sup>, Margaux Grandjean<sup>1</sup>, Paul Krusic<sup>6</sup>, Jonathan  
5 Palmer<sup>7</sup>

6 <sup>1</sup> School of Earth & Environmental Sciences, University of St. Andrews, UK

7 <sup>2</sup> School of Ecosystem and Forest Sciences, University of Melbourne, 500 Yarra Boulevard, Richmond 3121, Australia

8 <sup>3</sup> Tree-Ring Laboratory, School of Environment, The University of Auckland, Private Bag 92019, Auckland, New Zealand

9 <sup>4</sup> Lamont-Doherty Earth Observatory, Palisades, New York 10964, USA

10 <sup>5</sup> Department of Geological, Environmental, and Marine Sciences, Rider University, 2083 Lawrenceville Rd, Lawrenceville,  
11 NJ, 08648, USA

12 <sup>6</sup> Department of Geography, University of Cambridge, Cambridge, UK

13 <sup>7</sup> ARC Centre of Excellence in Australian Biodiversity and Heritage, School of Biological, Earth and Environmental  
14 Sciences, University of New South Wales, Sydney, NSW 2052, Australia

15 *Correspondence to:* Rob Wilson (rjsw@st-andrews.ac.uk)

16 **Abstract.** We evaluate a range of blue intensity (BI) tree-ring parameters in eight conifer species (12 sites) from Tasmania  
17 and New Zealand for their dendroclimatic potential, and as surrogate wood anatomical proxies. Using a dataset of ca. 10-15  
18 trees per site, we measured earlywood maximum blue intensity (EWB), latewood minimum blue intensity (LWB) and the  
19 associated delta blue intensity (DB) parameter for dendrochronological analysis. No resin extraction was performed,  
20 impacting low-frequency trends. Therefore, we focused only on the high-frequency signal by detrending all tree-ring and  
21 climate data using a 20-year cubic smoothing spline. All BI parameters express low relative variance and weak signal  
22 strength compared to ring-width. Correlation analysis and principal component regression experiments identified a weak and  
23 variable climate response for most ring-width chronologies. However, for most sites, the EWB data, despite weak signal  
24 strength, expressed strong coherence with summer temperatures. Significant correlations for LWB were also noted, but the  
25 sign of the relationship for most species is opposite to that reported for all conifer species in the Northern Hemisphere. DB  
26 results were mixed but performed better for the Tasmanian sites when combined through principal component regression  
27 methods than for New Zealand. Using the full multi-species/parameter network, excellent summer temperature calibration  
28 was identified for both Tasmania and New Zealand ranging from 52% to 78% explained variance for split periods (1901-  
29 1950 / 1951-1995), with equally robust independent validation (Coefficient of Efficiency = 0.41 to 0.77). Comparison of the  
30 Tasmanian BI reconstruction with a quantitative wood anatomical (QWA) reconstruction shows that these parameters record  
31 essentially the same strong high-frequency summer temperature signal. Despite these excellent results, a substantial  
32 challenge exists with the capture of potential secular scale climate trends. Although DB, band-pass and other signal  
33 processing methods may help with this issue, substantially more experimentation is needed in conjunction with comparative  
34 analysis with ring density and QWA measurements.

## 35 **1 Introduction**

36 The range of variables that are now routinely measured from the rings of trees, including width, stable isotopes, multiple  
37 wood anatomical properties and density, has increased substantially in recent years (McCarroll et al. 2002; McCarroll and  
38 Loader, 2004; Drew et al. 2012; von Arx et al. 2016; Björklund et al., 2020). However, our knowledge of the climatic,  
39 environmental, and physiological processes that modulate the year-to-year variability of these different tree-ring parameters  
40 is still far from comprehensive.

41

42 Since the early seminal work of Fritts et al. (1965), a well-known rule of thumb for ring-width (RW) based  
43 dendroclimatology is that trees sampled near their high elevation or latitude treelines will be predominantly temperature  
44 limited, while at lower elevations or latitudes, moisture limitation becomes the primary driver of growth (Fritts 1976;  
45 Kienast et al. 1987; Buckley et al. 1997; Wilson and Hopfmüller 2001; Briffa et al., 2002; Babst et al. 2013; St. George  
46 2014). Such targeted sampling is strategically vital in “traditional” dendroclimatology and robust reconstructions can be  
47 derived so long as tree-line sites are sampled where a single dominant climate parameter controls growth (Bradley 1999).  
48 However, the climatic influence on RW can be complex and there are many published studies where the relationship  
49 between RW and climate is shown to be temporally unstable and/or non-linear (Wilmking et al. 2020).

50

51 Ring density parameters, especially maximum latewood density (MXD), have been shown to provide substantially more  
52 robust estimates of past summer temperature compared to RW (Briffa et al., 2002; Wilson and Luckman, 2003; Esper et al.,  
53 2012; Büntgen et al., 2017; Ljungqvist et al., 2019). Density data may also retain a strong temperature signal at elevations  
54 below the upper treeline, minimising the non-linear influence of a changing tree-line elevation through time (Kienast et al.  
55 1987). The use of ring-density variables from lower elevation or latitude sites to reconstruct past hydroclimate is rare  
56 (Camarero et al. 2014, 2017; Cleaveland 1986; Seftigen et al. 2020) and is clearly an area demanding further attention.

57

58 The reconstructive value of tree ring stable isotopes (carbon and oxygen) appears to be less constrained for sites where  
59 climate does not limit growth and substantial potential exists from mid-latitude regions where traditional  
60 dendroclimatological approaches are less reliable (McCarroll and Loader, 2004; Loader et al. 2008; Young et al. 2015;  
61 Loader et al. 2020; Büntgen et al. 2021). However, within the mechanistic framework of stable isotopes, there is still much  
62 to explore regarding the complex associations between fractionation and climate for different species and across different  
63 ecotones.

64

65 The use of quantitative wood anatomical (QWA) parameters for dendroclimatology has gained traction in recent years due to  
66 improvements in measurement methodologies allowing for the development of well-replicated chronologies for multiple  
67 different anatomical variables (Drew et al. 2012; von Arx et al. 2016; Prendin et al., 2017; Björklund et al. 2020). The

68 strength of relationships between climate parameters and wood anatomical properties such as latewood cell wall thickness,  
69 tracheid radial diameter and microfibril angle is comparable to and can be stronger than maximum latewood density (Yasue  
70 et al., 2000; Wang et al., 2002; Panyushkina et al., 2003; Fonti et al., 2013; Allen et al. 2018).

71  
72 Despite the strong climate signal often noted in such non-RW tree-ring parameters, their procurement is expensive, often  
73 requires specialised equipment and experience, and is time consuming. Consequently, there are substantially less published  
74 data available for inspection and assessment. In recent years, blue intensity (BI) has been championed by many groups as a  
75 cheaper surrogate for maximum latewood density (Björklund et al., 2014a/b; Rydval et al., 2014; Wilson et al., 2014; Kaczka  
76 and Wilson 2021). In its common usage, BI measures the intensity of the reflectance of blue light from the latewood of  
77 scanned conifer samples so that a dense (dark) latewood would result in low-intensity values. MXD and BI essentially  
78 measure similar wood properties. Most studies that have directly compared MXD and latewood BI show no significant  
79 difference in the climate response of the two parameters (Wilson et al., 2014; Björklund et al. 2019; Ljungqvist et al., 2019;  
80 Reid and Wilson 2020). Though the acceptance of BI in dendrochronology was initially slow after the publication of the  
81 original concept paper (McCarroll et al. 2002), over the past decade many BI-based studies have been published (Kaczka and  
82 Wilson 2021). These studies have examined the use of BI as an ecological and climatological indicator in a variety of conifer  
83 species from several locations around the Northern Hemisphere (Campbell et al., 2007, 2011; Helama et al., 2013; Rydval et  
84 al., 2014, 2017, 2018; Björklund et al., 2014a/b; Wilson et al., 2014, 2017a, 2017b, 2019; Babst et al., 2016; Dolgova, 2016;  
85 Arbella et al., 2018; Buras et al., 2018; Fuentes et al., 2017; Kaczka et al., 2018; Wiles et al., 2019; Harley et al. 2021;  
86 Heeter et al. 2020; Reid and Wilson 2020; Davi et al. 2021).

87  
88 Only three studies that utilise BI data south of 30°N have been published. Buckley et al. (2018) explored the potential of  
89 reflectance parameters from the tropical conifer Fujian cypress (*Fokienia hodginsii*) from central Vietnam and found a  
90 significant positive relationship between earlywood maximum BI and December-April maximum temperature. Although a  
91 spring/early summer temperature signal is extant in Northern Hemisphere conifer minimum density data from temperature  
92 limited sites (Björklund et al. 2017), correlations are generally not as strong as the earlywood results detailed by Buckley et  
93 al. (2018). In the Southern Hemisphere, Brookhouse and Graham (2016) measured latewood BI from *Errinundra plum-pine*  
94 (*Podocarpus lawrencei*) samples taken from the Australian Alps and identified a strong inverse ( $r = -0.79$ ) relationship with  
95 August-April maximum temperatures, suggesting substantial potential for this species if long-lived specimens could be  
96 found. Finally, Blake et al. (2020) recently explored the climate signal in BI parameters measured from Silver pine (*Manoao*  
97 *colensoi*) samples growing on New Zealand's South Island and found strong significant relationships between both  
98 earlywood and latewood BI parameters and summer temperatures. Although the sign (positive) of the earlywood BI  
99 relationship with temperature agreed with results detailed in other studies (Björklund et al. 2017; Buckley et al. 2018), the  
100 latewood relationship was inverse to that detailed for Northern Hemisphere conifers (Briffa et al. 2002) and observed by  
101 Brookhouse and Graham (2016). This difference in latewood response begs the intriguing question as to whether some

102 Southern Hemisphere conifers may have evolved differently from their Northern Hemisphere counterparts, resulting in a  
 103 different anatomical and physiological response to climate.

104

105 Here we expand upon the pilot studies of Brookhouse and Graham (2016) and Blake et al. (2020) and explore the climate  
 106 signal of BI parameters from several key conifer species from Tasmania and New Zealand. To minimise nomenclature  
 107 confusion, we refer to the different BI parameters as earlywood blue intensity (EWB) and latewood blue intensity (LWB).  
 108 Based on ecophysiological theory (Buckley et al. 2018) we posit that EWB, derived from maximum intensity values of the  
 109 whole-ring reflectance spectrum, essentially provides a surrogate for mean lumen size of the earlywood cells, while LWB,  
 110 derived from minimum reflectance values, reflects the relative density (i.e. the proportion of cell wall to lumen area) of the  
 111 darker latewood cell walls. We further suggest these reflectance measures are useful surrogate measures of mean tracheid  
 112 diameter and cell wall thickness, which are proven to be excellent proxies of past climate (Allen et al. 2018; Björklund et al.  
 113 2019) but are laborious and expensive to measure directly. As well as undertaking a dendroclimatic assessment of multiple  
 114 BI parameters from different Australasian conifers, our analysis will also identify which species would be a good focus for  
 115 further BI and QWA measurement in the future. Improving terrestrial-based estimates of past temperature in the land-limited  
 116 Southern Hemisphere (Neukom et al. 2014) will only be achieved by enhancing the strength of the calibrated signal that until  
 117 recently has been characterized solely by ring-width data which generally express a weak temperature signal.

118

Site Name	Site code	Common name	Species	Latitude (S)	Longitude	Elevation (m)	No of series	No of trees	full period	period $\geq 3$ series
<b>TASMANIA</b>										
Race Spur	RCS	Celery Top pine	<i>Phyllocladus aspleniifolius</i>	41.29	145.44	500-550	16	14	1788-1995	1795-1995
L. Mackenzie	MCK	Pencil pine	<i>Athrotaxis cupressoides</i>	41.41	146.23	1116	15	15	1771-2007	1780-2007
Cradle Mountain	CM	Pencil pine	<i>Athrotaxis cupressoides</i>	41.40	145.57	1050	15	15	1787-2001	1789-2001
Mt Weld West / Trout Lake	MWWTRL	King Billy pine	<i>Athrotaxis selaginoides</i>	43.00	146.34	950	17	9	1781-1998	1785-1998
Mt Read - KBP	MRD	King Billy pine	<i>Athrotaxis selaginoides</i>	41.50	145.32	900	13	6	1770-2010	1778-2010
Mt Read - HP	MHP	Huon pine	<i>Lagarostrobos franklinii</i>	41.50	145.32	1000	22	16	781-2002	1238-2001
John Butters Power Station (King River)	BUT	Huon pine	<i>Lagarostrobos franklinii</i>	42.15	145.30	60	10	10	1773-2008	1798-2008
<b>NEW ZEALAND</b>										
Puketi	PKL	NZ Kauri	<i>Agathis australis</i>	35.15	173.45	180	13	10	1674-2001	1737-2001
Huapai	HUP	NZ Kauri	<i>Agathis australis</i>	36.48	174.3	100	17	13	1664-2007	1723-2006
Flagstaff	FLC	NZ Cedar	<i>Libocedrus bidwillii</i>	42.30	171.43	280	12	7	1774-2004	1776-2004
Ahaura	AHA	Silver pine	<i>Manoao colensoi</i>	42.23	171.48	244	12	12	1750-2012	1750-2012
Doughboy, Stewart Island	DPP	Pink pine	<i>Halocarpus biformis</i>	46.59	167.43	230	20	12	1767-2010	1777-2010

119

120

121 **Table 1: Chronology information for the seven Tasmanian and five New Zealand sites used in the study (see Figure 1).**

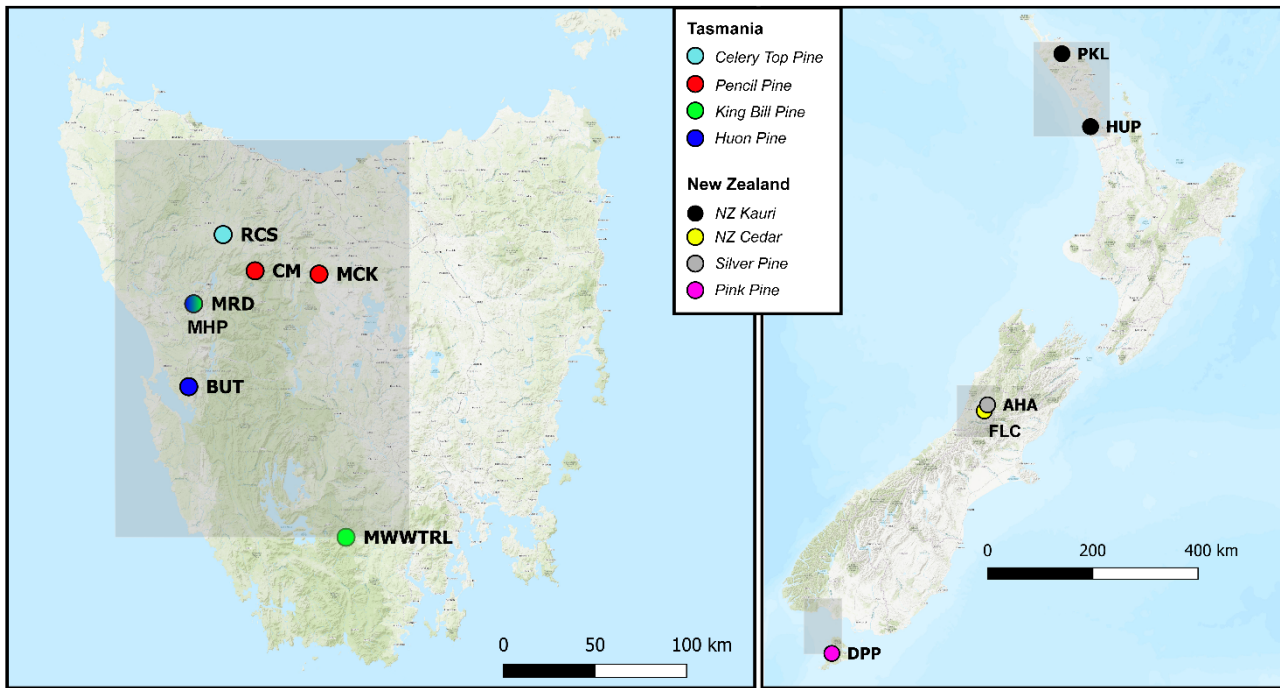
122

## 123 2 Data and Methods

124 Four tree species from Tasmania and four from New Zealand were targeted for analysis (Figure 1, Table 1) representing  
 125 conifer species that have not only been the focus of previous dendrochronological studies, but each has the potential to  
 126 produce climate proxy records substantially greater than 1000 years in length. Until recently, RW data were used for most

127 Australasian dendroclimatological studies, with calibration results never exceeding 40-45% explained variance. In Tasmania,  
128 the strongest calibration results for summer temperatures had been obtained using high elevation Huon pine (*Lagarostrobos*  
129 *franklinii* - Buckley et al. 1997; Cook et al. 2006) although some coherence was also found for Pencil pine (*Athrotaxis*  
130 *cupressoides*) and King Billy pine (*Athrotaxis selaginoides* - Allen et al. 2011; Allen et al. 2017). The study sites (Table 1)  
131 for Pencil pine (MCK and CM) and King Billy pine (MWWTRL and MRD) are located close to the upper timberline limit of  
132 these species and growth is expected to be controlled mostly by summer temperatures. Likewise, the high elevation Huon  
133 pine (MHP) site is also close to the upper treeline where summer temperature is the dominant response (Buckley et al. 1997).  
134 However, BUT is located at the lower end of the Huon pine elevational range within a riparian environment so temperature  
135 limitation is unlikely in a traditional sense. However, Drew et al (2012) identified strong summer temperature signals in  
136 latewood QWA data for this site. Celery Top (*Phyllocladus aspleniifolius*) RW data, however, express a complex non-linear  
137 relationship with climate along its species' elevational range and have not been used for dendroclimatic reconstruction  
138 (Allen et al. 2001). By contrast, summer temperature calibration experiments performed on measurement series of several  
139 wood anatomical properties (e.g. tracheid radial diameter, cell wall thickness and microfibril angle), as well as RW and ring  
140 density, from these same species, have shown substantial improvement over RW alone (Allen et al. 2018), although these  
141 QWA data have been more useful for hydroclimate reconstructions (Allen et al. 2015a/b). In New Zealand, RW-based  
142 summer temperature reconstructions have been developed from NZ Cedar (*Libocedrus bidwillii* - Palmer and Xiong 2004),  
143 Silver pine (*Manoao colensoi* - Cook et al. 2002, 2006) and Pink pine (*Halocarpus biformis* - D'Arrigo et al. 1996, Duncan  
144 et al. 2010) although ring density (Xiong et al. 1998 – Pink pine) and BI (Blake et al. 2020 – Silver pine) measured from the  
145 earlywood have produced stronger results. For this study, we specifically measured BI from samples used in previous,  
146 mostly RW-based dendroclimatic, studies where summer temperature was found to be the dominant climate signal - at least  
147 for NZ Cedar, Silver pine and Pink pine. The sites for these three New Zealand species are close to their southern  
148 (latitudinal) limits (especially the Stewart Island Pink pine site) which is thought to compensate, to some degree, for their  
149 modest elevational range (Table 1). Kauri (*Agathis australis*) is the longest-lived tree species in Australasia (Boswijk et al.  
150 2014) but only a few sites of reasonably mature trees exist. Previous analyses have identified a complex mixed response to  
151 both temperature and precipitation through the growing season (Buckley et al 2000, Fowler et al, 2000). However, it is  
152 notable that Kauri RW data express a strong stable relationship with indices of the El Nino Southern Oscillation (Cook et al.  
153 2006; Fowler et al. 2012).

154



155

156

157 **Figure 1: Location map (basemap ESRI 2021) of the tree-ring sites used in this study (see Table 1). Also indicated (grey boxes) are**  
 158 **the regional domains of the gridded CRU TS 4.03 temperature and precipitation data (Harris et al., 2014) used for analyses.**  
 159 **Tasmania: 145-147°E / 41-43°S; New Zealand: North: 173-175°E / 35-37°S; Central: 171-172°E / 42-43°S ; South: 167-168°E / 46-**  
 160 **47°S.**

161

162

163 In this study, we utilised tree cores sampled over the past three decades that has been prepared for RW measurement.  
 164 Considering the focus of this study is to assess the potential of BI parameters for enhancing dendroclimatic reconstruction,  
 165 and the fact that the samples were already mounted, no resin extraction was performed except for the Silver pine AHA site  
 166 (see Blake et al. 2020 for details). As many of the species are resinous by nature, this immediately imposes a potential  
 167 problem for measuring BI data, because any inhomogeneous resin-related discolouration will impact intensity values  
 168 (Rydval et al., 2014; Björklund et al., 2014a/b; Wilson et al. 2017b; Reid and Wilson 2020). Consequently, as the high-  
 169 frequency signal will only be minimally affected by discolouration (Wilson et al. 2017a), all analyses for this proof-of-  
 170 concept study will utilise only the high-pass fraction of the chronologies.

171

172 The mounted samples were re-sanded using fine grade (> 600 grit) sandpaper to remove decadal markings. Samples were  
 173 scanned at multiple institutions using different scanners and a range of resolutions from 1200 to 3200 DPI. RW and BI data  
 174 were generated using Coorecorder (Cybis 2016, <http://www.cybis.se/forfun/dendro/index.htm>) except for AHA

175 (WinDendro – see Blake et al. 2020). Regardless of image resolution, the CooRecorder BI generation “window” was set to  
176 roughly equate to two-thirds width of the sample while the window depth encompassed either the latewood or earlywood for  
177 each ring. The BI data were extracted following the method detailed in Buckley et al. (2018). For LWB, mean reflectance  
178 values were taken from the lowest 15% of the darkest pixels, while for EWB the mean of the brightest 85% of the pixels was  
179 used. Despite many of the samples being substantially older, most samples were measured only back into the 17<sup>th</sup> or 18<sup>th</sup>  
180 centuries (with site MHP (Table 1) being an exception), providing enough data to ensure robust calibration and validation  
181 over the instrumental period and to allow comparison with a temperature reconstruction from Tasmania based on QWA data  
182 (Allen et al. 2018). Parameters generated for analysis were RW, EWB and LWB. As the study focuses only on the high-  
183 frequency signal extant in the tree-ring data, the LWB data were not inverted as is the norm in Northern Hemisphere studies  
184 using data generated in CooRecorder (Rydval et al. 2014).

185

186 Perhaps the greatest limitation for BI data parameters is that any colour changes that do not represent year-to-year changes in  
187 wood anatomical features such as lumen size and cell wall thickness will impose a colour-related bias in the intensity  
188 measurements. Examples of non-anatomically related colour changes are those associated with the heartwood/sapwood  
189 transition, sections of highly resinous wood, or fungal staining. Björklund et al. (2014) proposed a statistical procedure that  
190 could correct for such colour changes. This procedure subtracts the LWB reflectance value from the EWB data producing a  
191 delta parameter (hereafter referred to as Delta BI - DB). Theoretically, DB should correct for common colour change biases  
192 between heartwood and sapwood and even resinous zones within the wood. To date, DB has been utilised successfully in  
193 only a few studies (Björklund et al., 2014a/b; Wilson et al., 2017b; Fuentes et al. 2017; Blake et al. 2020; Reid and Wilson  
194 2020). As no resin extraction was performed (except site AHA, Table 1) and all the species used for this study express a  
195 colour change from heartwood to sapwood, DB data will also be examined to explore its high-frequency dendroclimatic  
196 potential.

197

198 For some of the studied species, the heartwood/sapwood transition colour change is very sharp and pronounced in  
199 reflectance values (Figure A1), and inflexible detrending options could impose a systematic bias in the resultant detrended  
200 indices. As an extreme example, the heartwood/sapwood transition of the EWB raw mean non-detrended chronology for the  
201 CM Pencil pine site (Figure A2) cannot be tracked well with cubic smoothing splines (Cook and Peters 1981) of 200, 100 or  
202 even 50 years respectively. This is not surprising given that the smoothing spline, operating as a symmetric digital filter, is  
203 not well suited for dealing with abrupt changes in time series such as that observed in the CMewb chronology. In fact, the  
204 bias of low (pre-transition) and high (post- transition) index values are only minimised when a flexible 20-year spline is used  
205 because it better adapts to the observed discontinuity. However, this adaptability comes at the cost of losing potentially  
206 valuable >20-year variability in the time series. This is clearly undesirable and better ways of modelling and removing such  
207 discontinuities without the unwanted loss of lower-frequency variability are needed (see later discussion). Although less

208 flexible splines could be used for other species with a gradual or minimal colour change from heartwood to sapwood (Figure  
209 A1), a consistent approach to detrending was deemed prudent and therefore a 20-year spline was used for all datasets.  
210

211 The mean interseries correlation statistic (R<sub>BAR</sub>) is utilised to assess how many series are needed to attain an Expressed  
212 Population Signal value of 0.85 (Wigley et al. 1984; Wilson and Elling 2004). Previous research has shown that the common  
213 signal expressed by BI data can be rather weak (Wilson et al. 2014, 2017a/b, 2019; Kaczka et al. 2018; Wiles et al. 2019).  
214 We explore this phenomenon further with this multi-parameter/species network by using the coefficient of variation to help  
215 understand relative internal variance and covariance of the parameter chronologies.  
216

217 The climate signal expressed in the individual chronologies was initially explored using simple correlation analysis against  
218 monthly gridded (see Figure 1 for locations) CRUTS 4.03 temperature and precipitation data (Harris et al. 2014) for the  
219 periods 1902-1995, 1902-1950 and 1951-1995. Although the CRU TS data start in 1901, 1902 was the initial start year as  
220 correlations were performed over 20 months including the previous growing season while 1995 reflects the final common  
221 year for all tree-ring datasets (Table 1). The climate data were similarly detrended as the tree-ring data to ensure consistency.  
222 Unsurprisingly, as most of the study sites are located in temperature limited upper tree-line locations, correlations with  
223 monthly precipitation were weak, variable and temporally unstable for all species/parameter chronologies studies. The  
224 results are presented in the Appendix but are not discussed further (see Table A4a-d).  
225

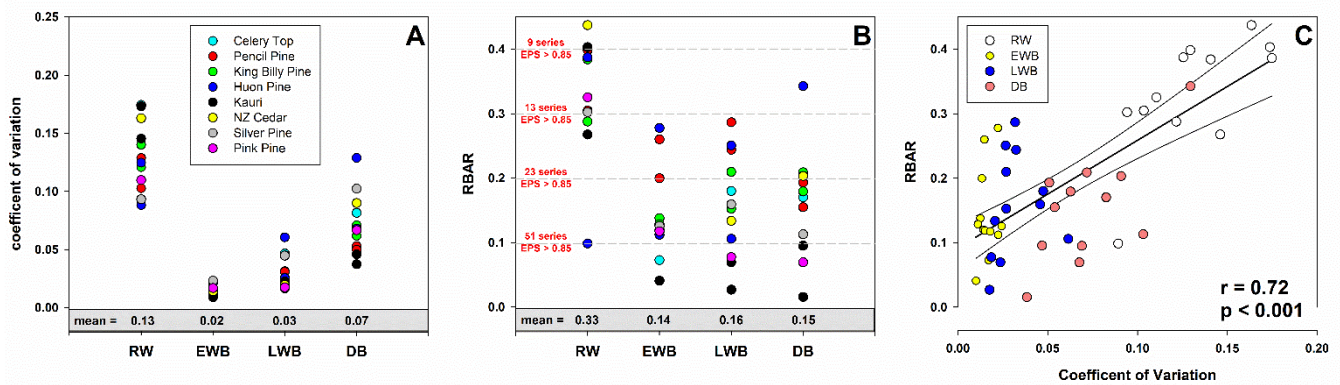
226 Principal component analysis (PCA) was used on varying subsets of chronologies for each region (i.e. all chronologies of the  
227 same parameter, or all parameters from a single species) to reduce the data to a few modes of common variance. Principal  
228 components that had both an eigenvalue > 1.0 and correlated significantly (95% C.L.) with the target instrumental data were  
229 entered into a stepwise multiple regression and calibrated against a range of seasonal temperatures. For New Zealand, the  
230 three CRU TS 4.03 grid boxes (Figure 1) were averaged to create a countrywide mean series. This was justified as the three  
231 inter-grid boxes mean correlation values between all tested seasons was 0.93 (STDEV = 0.01) suggesting there is a strong  
232 common temperature signal between North Island and southern South Island. PCA was also utilised to ascertain the optimal  
233 season for dendroclimatic calibration using the full chronology network for each country as well as exploring seasonal  
234 differences between parameters and species. Analyses were performed over the common period of all tree-ring and climate  
235 data (1901-1995) as well as early (1901-1950) and late (1951-1995) period calibration and verification. The Coefficient of  
236 Efficiency (CE - Cook et al., 1994) was used to validate the regression-based climate estimates.



## 238 3.1 Chronology variability and signal strength

239 Wilson et al. (2014), using upper tree-line temperature-sensitive spruce samples from British Columbia, noted lower mean  
 240 coefficient of variation (CV) values for LWB (0.05) compared to RW (0.28) and MXD (0.19). Common signal strength was  
 241 strongest for the MXD data (RBAR = 0.42) while RW and LWB expressed similar but lower values (0.30). For the  
 242 Australasian detrended data, overall, RW data express higher relative variance (mean CV = 0.13) followed by DB (0.07),  
 243 LWB (0.03) and EWB (0.02 – Figure 2a). The range in values for RW (0.09 – 0.17) and DB (0.04 - 0.13) are greater than  
 244 LWB (0.02 - 0.06) although there is overlap in the range of DB and LWB. The EWB data express a significantly narrower  
 245 range (0.01 - 0.02). RBAR values for the four different parameter groups generally return a stronger common signal for RW  
 246 (mean = 0.33) compared with EWB (0.14), LWB (0.16), and DB (0.15 – Figure 2b). Therefore, following traditional  
 247 methodologies to assess signal strength, more BI series are needed than RW to attain a robust chronology. On average across  
 248 all sites, to attain an EPS value of at least 0.85 (Wigley et al. 1984), 14 series would be needed for RW, while 44, 47 and 58  
 249 series would be needed for EWB, LWB and DB respectively. This weaker common signal of the BI parameters has been  
 250 noted before (Wilson et al. 2014, 2017a/b, 2019; Kaczka et al. 2018; Wiles et al. 2019; Blake et al. 2020) and is also noted in  
 251 QWA data from Tasmania (Allen et al. *in prep*). The common signal is particularly weak for Celery Top and Kauri (EWB)  
 252 and Pink pine and Kauri (LWB and DB – see Table A1 for detailed values).

253



254

255 **Figure 2: A. Coefficient of variation (CV) of the 20-year spline detrended chronologies; B: mean inter-series correlation (RBAR) of**  
 256 **the 20-year spline detrended series. Horizontal dashed lines denote the number of series needed for that particular RBAR value to**  
 257 **attain an EPS of 0.85; C: Scatter plot of CV versus RBAR with linear regression.**

258

259 A scatter plot of the CV and RBAR data (Figure 2c) suggests that the common signal expressed by these chronologies is  
 260 partly a function of the relative variance of the time-series ( $r = 0.72$ ,  $p < 0.001$ ). Although the range in RBAR values for the  
 261 EWB and LWB data suggests some uncertainty in this observation (see also Table A1), these results imply that the relatively

262 low variation of values around the mean for the BI parameters suggests that any anomalous colour staining on the wood that  
263 does not reflect the true wood properties being measured could have a substantial impact on the chronology common signal.  
264 However, it should be emphasised that a weak common signal and low EPS value does not necessarily result in a weak  
265 climate signal (Buras 2017).

### 266 3.2 Climate response

267 The strength of correlations between the RW chronologies and mean monthly temperatures vary in sign and strength across  
268 species. Over the full 1902-1995 period (Table 2), the Tasmanian MWWTRL (King Billy pine) and MHP (high elevation  
269 Huon pine) sites express significant positive correlations with September-February and January-February respectively,  
270 which are broadly time stable (Table A3a). RCS (Celery Top pine), MCK (Pencil pine) and MRD (King Billy pine) show  
271 inverse correlations with late summer temperatures of the previous year. Of the New Zealand sites, PKL (Kauri) has negative  
272 correlations for many months from winter through to the summer, while AHA (Silver pine) and DPP (Pink pine) correlate  
273 positively with December-April and September- November.

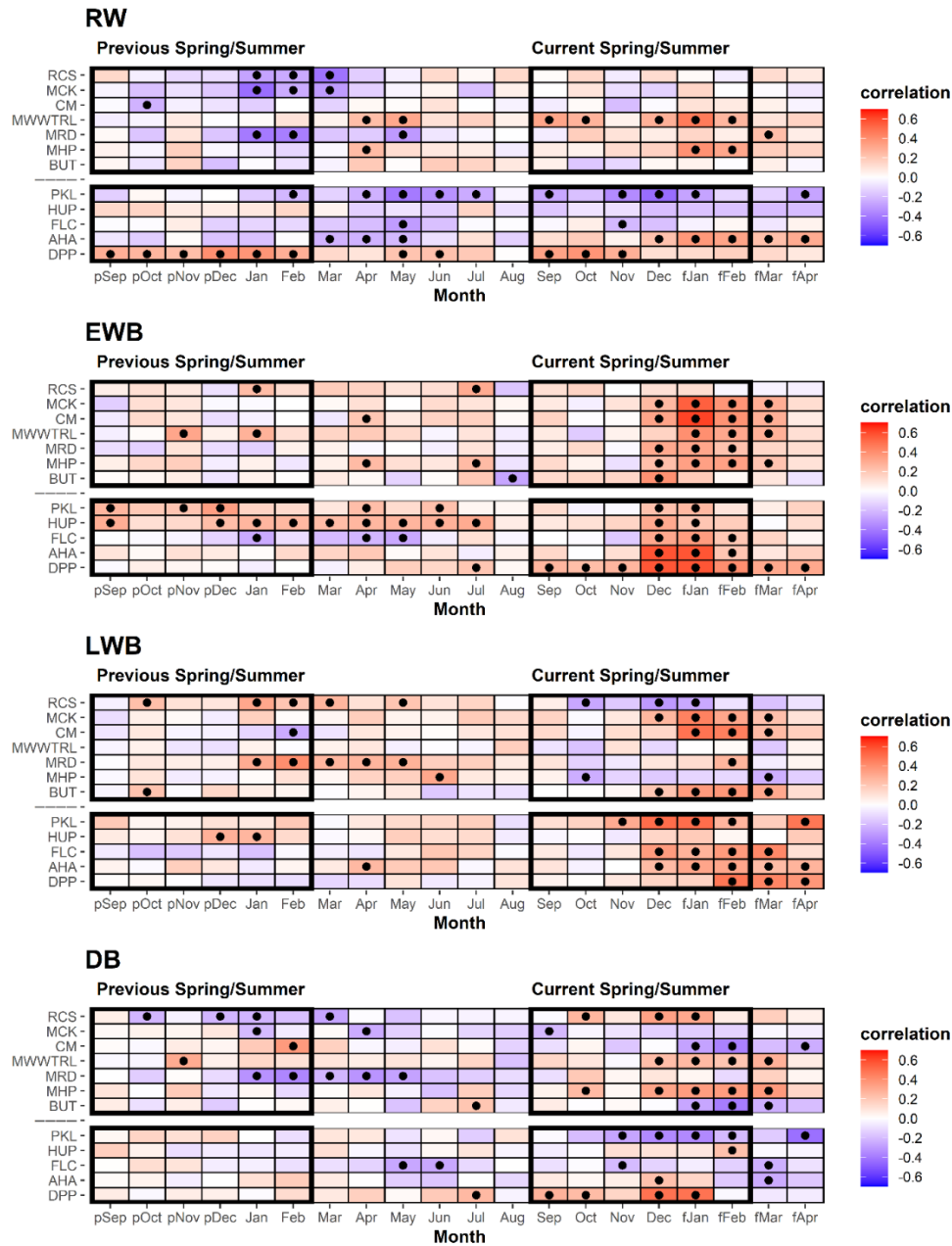
274

275 Correlations between the EWB chronologies and mean temperatures are surprisingly consistent for most sites although  
276 correlations for RCS (Celery Top pine) and BUT (low elevation Huon pine) are weak. Almost all site chronologies correlate  
277 positively with the summer months for the current season – December through to March (Tasmania) and December-February  
278 (New Zealand). The King Billy pine and Kauri sites express narrower (MMWTRL, MRD, PKL, and HUP) response  
279 windows while DPP (Pink pine) is wider (Table 2). Although these relationships appear generally time stable, the Tasmanian  
280 sites correlate more strongly with the narrower January-February season for 1902-1950 compared to the later post-1951  
281 period (Table A3b). Significant correlations with winter and prior year temperatures are weaker and less consistent than for  
282 current spring/summer. Overall, the consistent and strong correlations of EWB with summer temperatures are extremely  
283 encouraging and show great promise for enhancing RW-based temperature reconstruction for both regions.

284

285 Significant relationships between LWB and summer and early Autumn temperatures are generally noted, although the results  
286 are less consistent than those for EWB. Both RCS (Celery Top) and high elevation Huon pine (MHP) express negative  
287 correlations that are in line with the positive MXD/temperature relationships noted in the Northern Hemisphere as the LWB  
288 data are not inverted. Excluding MMWTRL (King Billy pine) and HUP (Kauri), which do not have any significant  
289 correlations with temperature in the growing season, all the LWB chronologies express positive correlations with summer  
290 and early autumn temperatures. This antithetic behaviour is not a new observation and has been noted by Drew et al. (2012),  
291 O'Donnell et al. (2016), Blake et al. (2020) for latewood anatomical parameters and LWB data, but these new results suggest  
292 that this physiological phenomenon is not based on a chance occurrence of a single species and is consistent between several  
293 Australasian conifer tree species (Pencil pine, Huon pine (low elevation), Kauri, NZ Cedar, Silver pine and Pink pine). Blake

294 et al. (2020) explained the inverse LWB relationship as a reduction in the duration of secondary cell wall thickening in  
 295 warmer years. Such “emergent” surprising results (Cook and Pederson 2011) clearly need further research and testing.  
 296



297  
 298 **Table 2: Correlation response function analysis results for the different TR parameter chronologies with CRU TS temperatures.**  
 299 **Analysis undertaken over the 1902-1995 period (see supplementary figure S3 for correlations for split periods 1902-1950, 1951-**  
 300 **1995). The upper block is for the Tasmanian sites, while the lower block is New Zealand. See Table 1 for site code names and**  
 301 **species. Black dots denoted correlations significant at the 95% C.L.**

303 The DB chronologies express a range of responses to temperature that are all generally weaker than for EWB and LWB  
304 (Table 2). Significant positive correlations with summer temperatures are found for RCS (Celery Top), MMWTRL (King  
305 Billy pine), MHP (Huon pine), and DPP (Pink pine). HUP (Kauri) and AHA (Silver pine) also express some weak positive  
306 summer temperature coherence. Negative correlations are noted for CM (Pencil pine), BUT (low elevation Huon pine), PKL  
307 (Kauri) and FLC (NZ Cedar). However, many of these correlations are not temporally stable when compared over the 1902-  
308 1950 and 1951-1995 periods (Table A3d). Current theory suggests that DB should perform well when EWB and LWB  
309 parameters are weakly correlated and express different earlier and later seasonal climate responses (Björklund et al., 2014).  
310 However, the results herein indicate that this simple hypothesis does not consistently apply in this multi-species study. For  
311 example, the EWB and LWB data for the Pink pine DPP site express different early (Sep-April) and late (Feb-Apr) seasonal  
312 responses with temperatures (Table 2), but still show a reasonably high inter-parameter correlation (0.60, Table A2) although  
313 this is partly expected as the response windows overlap. However, the DB data still expresses a significant and strong  
314 response with summer temperatures, although marginally weaker than the EWB response. On the other hand, DB for the  
315 Pencil pine sites (MCK and CM) behaves more like conifers in the Northern Hemisphere (Björklund et al., 2014; Wilson et  
316 al. 2017b), with significant correlations noted for both EWB and LWB with summer temperatures, but, likely due to the high  
317 inter-parameter correlation (0.57 and 0.68), the DB data express weak, or even inverse correlations with summer  
318 temperatures. Overall, the DB results are mixed and disappointing. This parameter theoretically could minimise the colour  
319 bias of the darker to lighter colour heartwood/sapwood transition (Figure A1) but, for the data used herein, as the high-  
320 frequency signal often portrays a mixed or weak signal with temperature, it suggests that the DB parameter might not be a  
321 valid approach to address the heartwood/sapwood transition bias. These results suggest that alternative approaches to using  
322 DB may need to be explored to minimise the impact of the heartwood/sapwood change noted in most of the species used in  
323 this study.

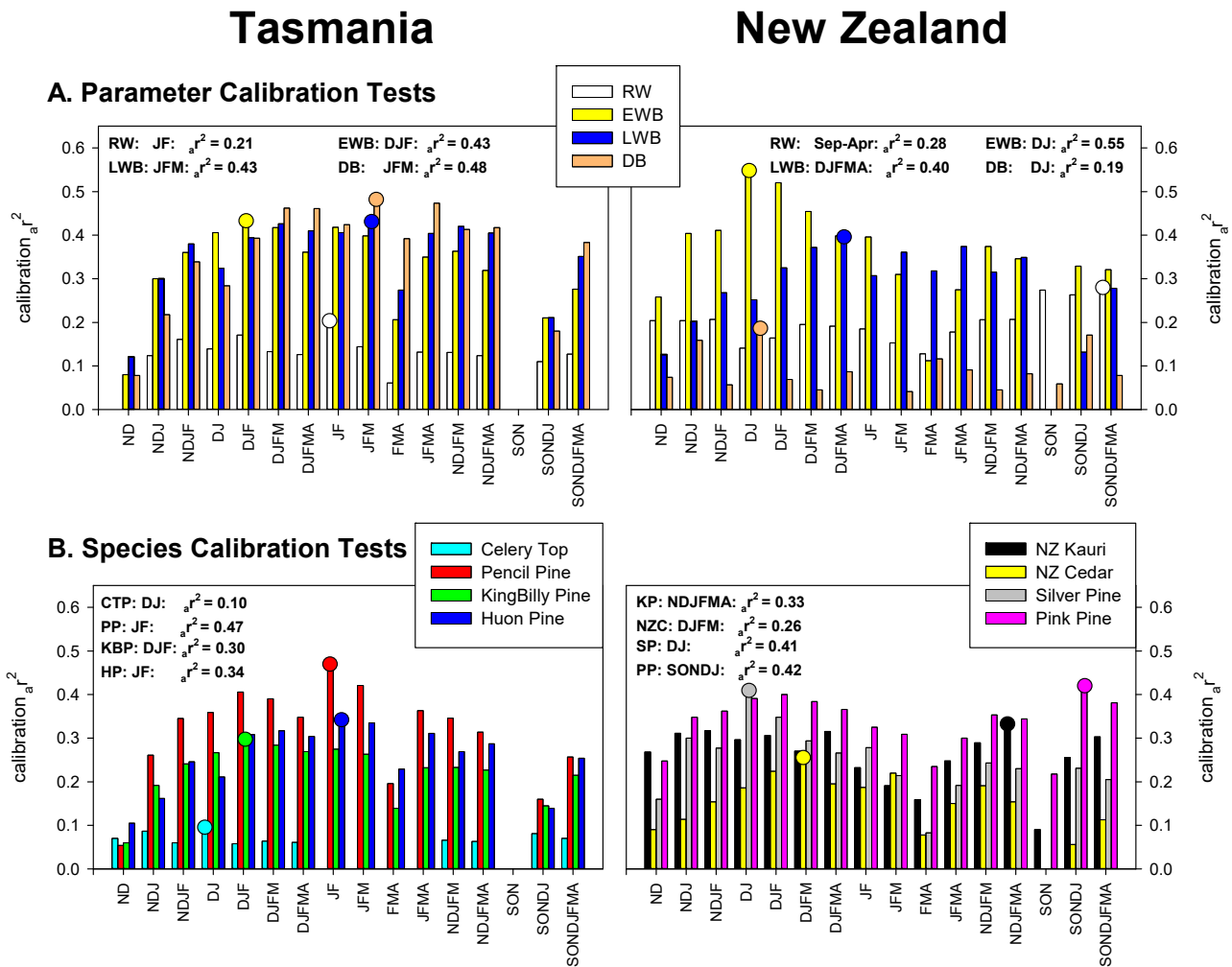
### 324 **3.3 Parameter and species-specific principal component calibration tests**

325 The previous section detailed that temperature is the predominant climate signal expressed across the Tasmanian and New  
326 Zealand RW and BI data studied herein (Figures 3, A3a-d). Only weak coherence with precipitation was found (Table A4a-  
327 d). To further explore the climate response, principal component regression calibration (1901-1995) experiments with  
328 seasonal temperature were performed to ascertain which combination of BI parameters and species express the strongest  
329 climate signal and therefore should be the focus for future research – including refined BI measurement and/or QWA  
330 measurement.

331

332 For Tasmania, the PCA identifies three (RW), two (EWB), two (LWB) and two (DB) principal components respectively.  
333 Each BI parameter PC regression explains > 40% of the temperature variance while RW is substantially weaker at 21%  
334 (Figure 3a). Both EWB and LWB explain 43% of the December-February and January-March variance respectively - these

335 seasons being biologically logical with respect to the earlier seasonal start for EWB and later end for LWB. Despite the site-  
 336 specific DB data correlating with temperature more weakly than EWB and LWB (Table 2), their multivariate combination  
 337 calibrates better (48%) with January-March temperatures. Although this is an encouraging result as DB may theoretically  
 338 correct for colour related biases, the mix of positive and negative zero-order correlations with temperature (Table 2) suggest  
 339 that some caution will be needed if such data are used to capture more secular scale information.  
 340



341  
 342 **Figure 3: PC regression calibration (1901-1995) experiments for parameters (all species) (A) and species (all variables) (B). A**  
 343 **range of temperature seasonal targets are used with the strongest seasonal calibrations highlighted with circles.**

344  
 345 For New Zealand, PCA identifies 3, 2, 2 and 3 significant principal components for RW, EWB, LWB and DB respectively.  
 346 EWB calibrates very strongly (55%) with December-January temperatures while LWB explains 40% of the broader

347 December-April season (Figure 3a). Alone, RW explains 28% of the temperature variance but for a broad September-April  
348 season which reflects the variable site-specific responses of PKL, AHA and DPP (Table 2). The DB data calibrate poorly  
349 explaining only 19% of the December-January temperature variance.

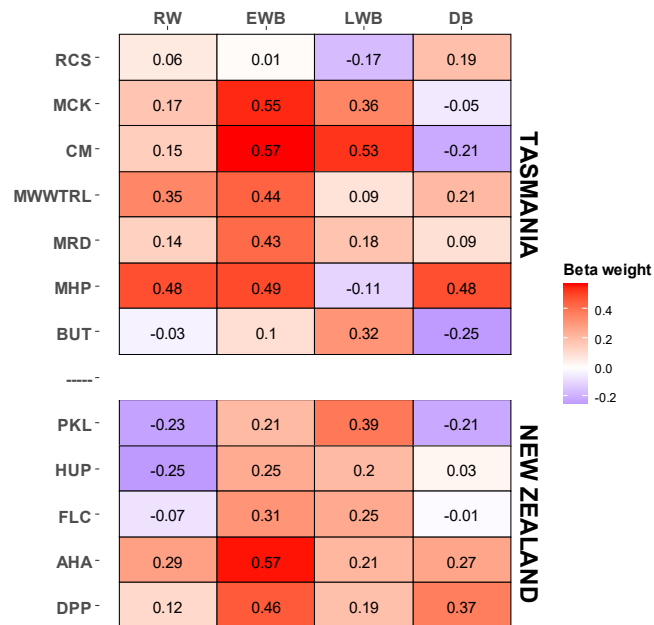
350

351 Of all the species tested, Tasmanian Pencil pine returns the strongest calibration (47%) with January-February temperatures  
352 (Figure 3b) although New Zealand Silver pine and Pink pine also calibrate reasonably with 41% (December-January) and  
353 42% (September-January). It should be noted that two Pencil pine sites were used (Table 1) compared to only one each for  
354 Silver pine and Pink pine which likely will influence these results. King Billy pine, Huon pine and Kauri explain 30%  
355 (December-February), 34% (January-February) and 33% (November-April) respectively of the temperature variance with  
356 New Zealand cedar still showing some reasonable coherence (26%) for December-March. Celery Top is the weakest species  
357 explaining only 10% of the December-January temperature variance.

### 358 **3.4 Region-wide calibration and validation**

359 A multi-site, multi-species approach to dendroclimatology can improve overall calibration even if some of the sampled sites  
360 and species are not located close to climate limited treeline ecotones (Alexander et al. 2019). Herein we have an opportunity  
361 to pool all the data for each country to create combined multi-species and multi-parameter regional reconstructions. As the  
362 optimal season for calibration varies as a function of species and parameter (Figure 3), initial PC regression experiments,  
363 using all chronologies from each of the two regions, were performed. For each of these models, all PCs with an eigenvalue  
364  $> 1.0$  were entered into the regression model. January-February (JF) temperature was identified as the overall optimal season  
365 for Tasmania while December-January (DJ) provided the strongest calibration for New Zealand. Forcing all variables into  
366 the PC regression model also provides an opportunity to identify the importance of each species parameter towards the  
367 development of regional reconstructions. The beta weights (Cook et al. 1994) from the regression modelling (Table 3)  
368 clearly show the strong influence of the EWB parameters in the multiple regression model, especially from Pencil pine  
369 (MCK and CM) and Silver pine (AHA) although strong beta weights are also noted for King Billy pine (MDR), Huon pine  
370 (MHP) and Pink pine (DPP). Other parameters that provide useful information in the modelling are RW (King Billy pine  
371 (MWWTRL) and Huon pine (MHP)), LWB (Pencil pine (MCK, CM), Huon pine (BUT) and Kauri (PKL)) and DB (Huon  
372 pine (MHP) and Pink pine DPP)). These results are consistent with the correlation response function analysis (Table 2), but  
373 it must be emphasised that the results shown in Table 3 are related to specific seasons (JF for Tasmania and DJ for New  
374 Zealand) and may not reflect the optimal season for individual species or parameters (Figure 3).

375



376

377

378 **Table 3: PC regression calibration (1901-1995) beta weights using all parameter and species data. The Tasmanian modelling was**  
 379 **performed against January-February temperatures while New Zealand was with December-January.**

380

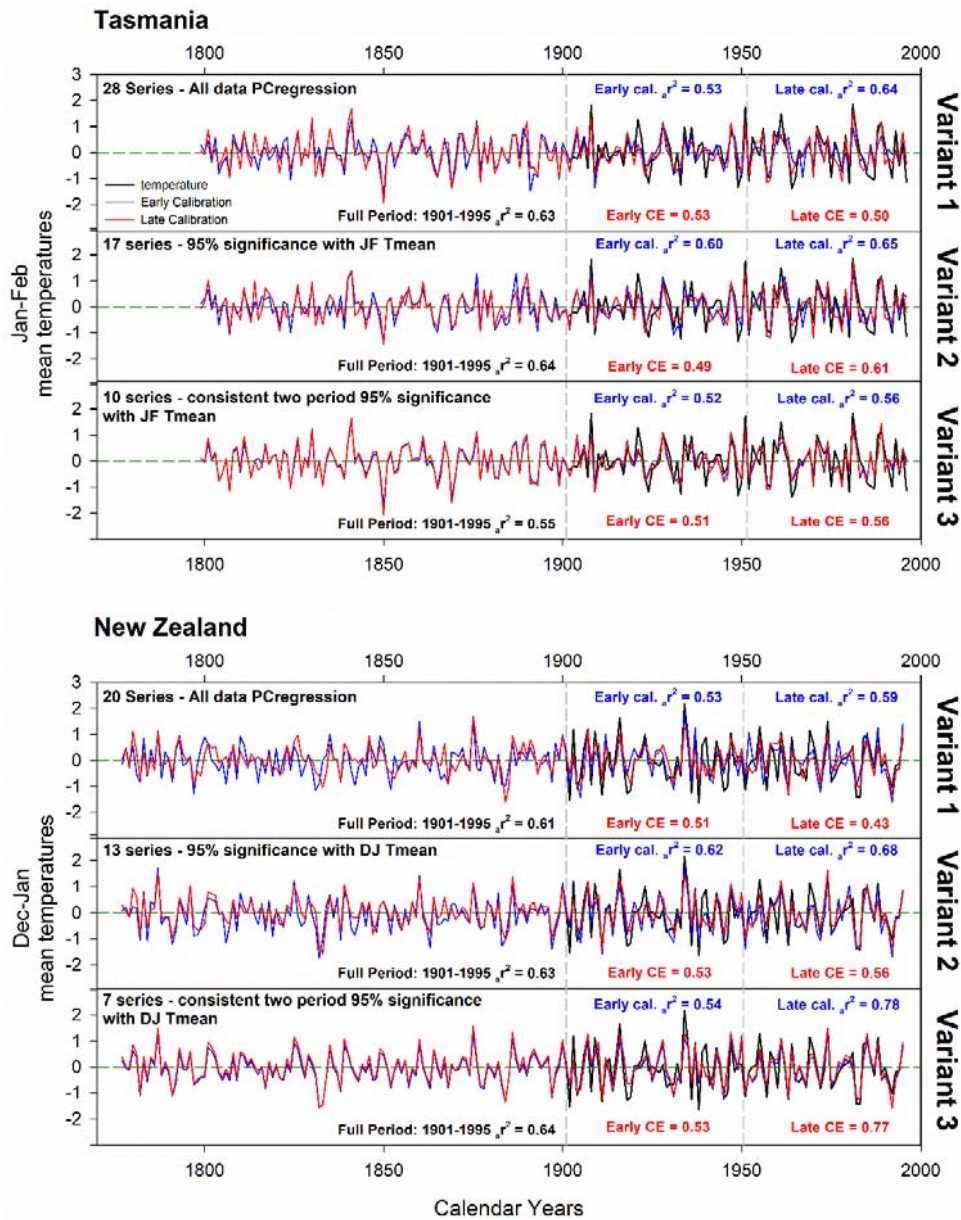
381

382 For the final countrywide calibration and validation experiments, three PC regression approaches were used, each reflecting  
 383 more stringent screening procedures; (1) as already detailed above - all data entered into PCA and PCs with an eigenvalue >  
 384 1.0 that correlated significantly (95%) with the instrumental target were entered as possible candidates into a stepwise  
 385 multiple regression; (2) same as (1) but chronologies were initially screened for significant correlation with the full period  
 386 instrumental target before PCA; (3) similar to previous variants, but significant consistent correlations between the  
 387 chronologies and the instrumental target for both the 1901-1950 and 1951-1995 periods were required.

388

389 For Tasmania, the initial 28 parameter chronologies were reduced to 17 and 10 respectively via the two more stringent  
 390 screening procedures while the 20 initial chronologies from New Zealand were reduced to 13 and 7 respectively (Figure 4).  
 391 Full period (1901-1995) calibration is excellent for all versions with the Tasmanian variants 1 and 2 expressing 63-64% of  
 392 the JF temperature variance, reducing to 55% for variant 3. The New Zealand data return similarly good results with 61-64%  
 393 of the DJ temperature variance being explained by all variants. Split period calibration and validation are equally good for all  
 394 variants with the Tasmanian variants explaining 52-65% of the variance for all early/late period calibration while CE ranges  
 395 from 0.49-0.61. Similar results are obtained for New Zealand with calibration adjusted  $r^2$  ( $a_r^2$ ) and CE values ranging from

396 0.53-0.78 and 0.43-0.77 respectively. For both countries, calibration and validation are marginally stronger for the later  
 397 1951-1995 period which might suggest some degree of uncertainty in the instrumental period in the early part of the 20th  
 398 century.  
 399

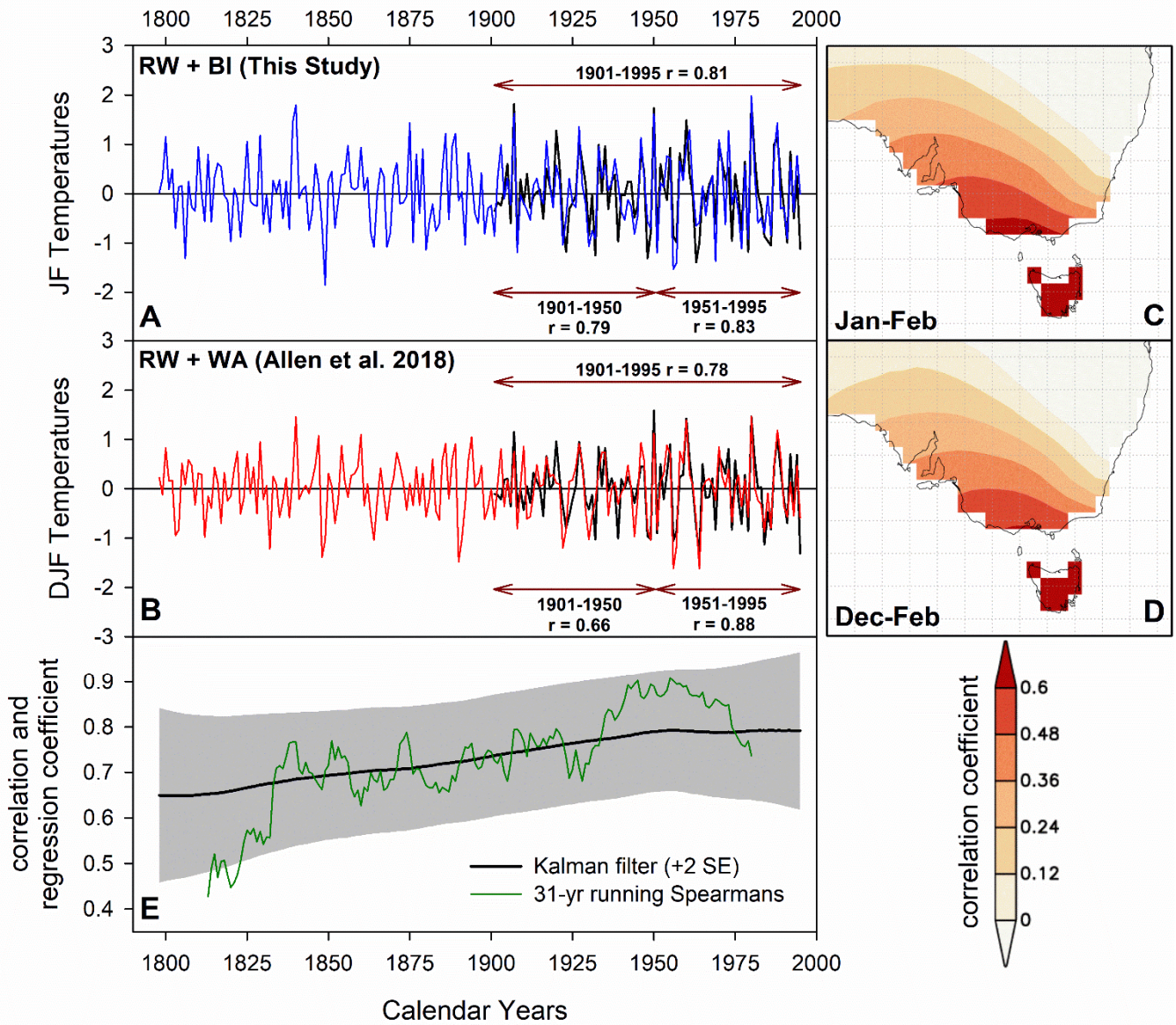


400

401

402 **Figure 4: Principal component regression results using all data (Variant 1), full period (1901-1995) screened data (Variant 2), and**  
 403 **two-period screening (Variant 3). Split period calibration and validation were performed over 1901-1950 and 1951-1995.**





404

405

406 **Figure 5: A: Variant 2 (full period screened) Tasmanian JF temperature RW+BI parameter-based reconstruction with CRU TS**  
 407 **temperature data. Pearson's correlation is shown for 1901-1995, 1901-1950 and 1951-1995 period; B: As A, but for Allen et al.**  
 408 **(2018) RW+WA based Tasmanian DJF temperature reconstruction. These data have also been high-pass filtered using a 20-year**  
 409 **cubic smoothing spline; C + D: Spatial correlations (1841-1995) between each reconstruction and similarly detrended Berkeley**  
 410 **gridded data for the Jan-Feb and Dec-Feb seasons respectively; E: Running 31-year Spearman's rank correlation and Kalman**  
 411 **filter analysis (Visser and Molenaar 1988).**

412

413 Overall, the temperature reconstruction experiments for both Tasmania and New Zealand (Figure 4) return excellent results  
414 with overall calibration  $r^2$  values well above 0.60. Although no QWA data exist yet for New Zealand, Allen et al. (2018)  
415 recently produced a range of PC regression-based Tasmanian summer temperature reconstructions from a network of 58  
416 chronologies using RW and QWA (mean tracheid radial diameter, mean cell wall thickness, mean density and microfibril  
417 angle). These variables were measured using the SilviScan system (Evans, 1994) from the same four Tasmanian tree species  
418 used herein using samples from the same region, but from more sites. Strong calibration results explaining 50-60% of the  
419 temperature variance and robust validation were also noted in their analyses. We compare our full period screened  
420 temperature reconstruction (Variant 2, Figure 4 – representing the most used data screening approach in dendroclimatology)  
421 with a high-pass filtered (20-year spline) version of Allen et al.’s (2018) “Berkeley all-data” reconstruction variant (Figure  
422 5). Both reconstructions correlate similarly with the CRU TS temperature data (1901-1995: RW/BI  $r = 0.81$  (JF) and  
423 RW/WA  $r = 0.78$  (DJF) – Figure 5a/b) although the BI-based reconstruction expresses a slightly more stable response with  
424 temperatures over the 1901-1950 and 1951-1995 periods ( $r = 0.79$  and  $0.83$  vs  $0.66$  vs  $0.88$ ). However, as the BI-based  
425 reconstruction was calibrated against these CRU TS data, this slight difference may simply reflect the optimised PC  
426 regression fit to one instrumental dataset over another. Equivalent split period correlations using the Berkeley temperature  
427 data (Rohde et al. 2013), as used by Allen et al. (2018), are  $0.82/0.86$  (RW/BI) and  $0.77-0.90$  (RW/WA).

428

429 Correlation with the Berkeley data over the 1841-1900 period, shows that coherence is weaker but similar between Allen et  
430 al.’s (2018) and this study ( $0.54$  and  $0.66$ ). The spatial representation of the reconstructed temperature signal in both datasets  
431 is almost identical when using linearly detrended Berkeley gridded temperature data (Rohde et al. 2013) even when  
432 including data back to 1841 (Figure 5c/d). Both reconstructions are strongly correlated with each other (Pearson’s  $r = 0.75$ ,  
433 1798-1995) although this coherence weakens back in time as evidenced by both a running 31-year Spearman’s rank  
434 correlation and Kalman filter (Visser and Molenaar 1988), showing a peak coherence in the 20th century that decreases back  
435 towards the early part of the 19th century (Figure 5e). This likely represents the decrease in sample replication through time  
436 in some BI-based datasets (MWWTRL and BUT) used in this study (Figure A1). Overall, the BI data, at least for Tasmania,  
437 basically express the same high-frequency signal as the WA data used in Allen et al. (2018) and the results herein suggest  
438 that BI parameters could provide excellent proxies of past growing season temperatures. However, for their potential to be  
439 truly realised, the heartwood/sapwood colour change and other discolouration issues need to be overcome.

#### 440 **4 Conclusions and future research directions**

441 In this study, we measured a range of blue intensity parameters from eight conifer species from Tasmania and New Zealand  
442 to ascertain whether the use of EWB, LWB and/or DB can improve upon previous RW-only based dendroclimatic  
443 reconstructions that explain about 40-45% of the temperature variance. No attempt to remove resins was made for this proof-  
444 of-concept study. Therefore, due to the impact on intensity-based parameters of resins and heartwood/sapwood colour

445 changes on the wood, we detrended the chronologies and climate data using a very flexible spline (20-years) to focus only on  
446 the high-frequency signal. Metrics denoting signal strength (RBAR and EPS) indicated a very weak common signal in the BI  
447 parameters (mean RBAR range 0.14 – 0.16, Figure 2b) compared to the RW data (mean RBAR = 0.33) which appeared to be  
448 partly related to the relative variance in these datasets. The EWB data in particular exhibit very low variability which may  
449 mean that any colour variation in the wood that does not reflect true year-to-year wood anatomical variance may have a large  
450 impact on such data, thus weakening the common signal.

451

452 Despite the weak common signal expressed by the BI parameters, the climate signal extant in these data is very strong,  
453 especially EWB. When all parameters are combined using PC regression, depending on the period used, 52-78% of the  
454 summer temperature variance can be explained (Figure 4). This is generally greater than the norm for Northern Hemisphere  
455 based MXD/BI-related temperature reconstructions (Wilson et al. 2016), although admittedly, the results in this study are  
456 focused only on the high-frequency fraction of the data. These strong calibration results are driven mainly by EWB data  
457 from Pencil pine, high elevation Huon pine and King Billy pine (Tasmania) and Silver pine, Pink pine and cedar (New  
458 Zealand) although useful information was also identified in LWB (Pencil pine, low elevation Huon pine, Kauri and cedar),  
459 DB (high elevation Huon pine and Pink pine) and RW (high elevation Huon pine – Table 3). However, the relationship of  
460 LWB for most species with summer temperatures is opposite to that observed in the Northern Hemisphere and further study  
461 is needed to assess the physiological processes leading to this inverse relationship in these particular Southern Hemisphere  
462 conifers.

463

464 The similarity of the Tasmanian multi-TR-proxy reconstruction with a reconstruction heavily dependent on QWA data  
465 (Allen et al. (2018) - Figure 5) clearly highlights that the BI and WA data express similar wood properties. This is a highly  
466 encouraging result for the utilisation of BI as it is quicker and cheaper to produce than QWA data. However, the “elephant in  
467 the room” is whether robust low-frequency information can be extracted from BI-based parameters or is it an analytical  
468 methodology that ultimately will be relevant only for decadal and higher frequencies. It is unlikely that the  
469 heartwood/sapwood colour change (both sharp and gradual – Figure A1), expressed by most of the tree species used in this  
470 study, can be fully removed by resin extraction alone. Some success at overcoming heartwood/sapwood colour bias using  
471 DB has been shown for some Northern Hemisphere conifer species (Björklund et al., 2014a/b; Wilson et al., 2017b; Fuentes  
472 et al. 2017; Reid and Wilson 2020), but the DB results detailed herein (Table 3, Figures 2- 4) suggest that DB may not  
473 always provide a robust solution to the issue.

474

475 Other statistical approaches have been used to overcome the colour bias using either contrast adjustments (Björklund et al.,  
476 2014b; Fuentes et al., 2017) or band-pass approaches where the low-frequency signal is derived from the RW data and the  
477 high frequency is driven by the BI data (Rydval et al., 2017) but further experimentation is needed. We hypothesise that  
478 relatively sharp changes in colour intensity measures related to the heartwood/sapwood transition can be viewed

479 conceptually in a similar way to how endogenous disturbances affect ring-width parameters over time (Cook 1987). Similar  
480 to the progress in developing growth release detection methods to reconstruct canopy disturbance histories of forests  
481 (Altman 2020, Trotsiuk et al. 2018), radial growth averaging (Lorimer and Frelich 1989) or time series methods  
482 (Druckenbrod et al., 2013; Rydval et al. 2015) could be used to identify and remove the colour bias signature resulting from  
483 the change in physiology from heartwood to sapwood. However, to facilitate such signal processing methods, more studies  
484 are needed to directly compare both MXD and QWA data with BI parameters to understand the secular trend biases in these  
485 light intensity parameters. At the very least, the results detailed herein, based on a limited number of sites per species, show  
486 that BI parameters can be used to identify those species that should be targeted for more costly and time-consuming  
487 analytical methods such as QWA measurement.

SITE code	Mean value	CV	RBAR	n-EPS (0.85)
<b>TASMANIA</b>				
RCSrw	0.72	0.17	0.39	9.0
RCSewb	1.02	0.02	0.07	70.2
RCSlwb	0.58	0.05	0.18	25.6
RCSdb	0.45	0.08	0.17	27.3
MCKrw	0.75	0.13	0.40	8.5
MCKewb	1.19	0.01	0.20	22.5
MCKlwb	0.78	0.03	0.25	17.4
MCKdb	0.40	0.05	0.16	30.6
CMrw	0.71	0.10	0.31	12.9
CMewb	1.22	0.01	0.26	16.0
CMlwb	0.84	0.03	0.29	14.0
CMdb	0.36	0.05	0.19	23.5
MWWTRLrw	0.59	0.12	0.29	14.0
MWWTRLewb	1.23	0.01	0.14	34.9
MWWTRLlwb	0.82	0.03	0.15	31.1
MWWTRLdb	0.33	0.06	0.18	25.7
MRDrw	0.60	0.14	0.38	9.1
MRDewb	1.28	0.01	0.13	37.9
MRDlwb	0.88	0.03	0.21	21.2
MRDdb	0.40	0.07	0.21	21.3
MHPrw	0.36	0.13	0.39	8.9
MHPewb	1.06	0.02	0.28	14.7
MHPlwb	0.82	0.03	0.25	16.8
MHPdb	0.24	0.13	0.34	10.8
BUTrw	0.99	0.09	0.10	50.8
BUTewb	1.18	0.02	0.11	44.1
BUTlwb	0.63	0.06	0.11	47.0
BUTdb	0.58	0.07	0.10	52.9
<b>NEW ZEALAND</b>				
PKLrw	1.16	0.17	0.40	8.4
PKLewb	1.17	0.01	0.12	40.9
PKLlwb	0.83	0.02	0.07	73.7
PKLdb	0.34	0.05	0.10	52.6
HUPrw	1.39	0.15	0.27	15.4
HUPewb	1.03	0.01	0.04	126.7
HUPlwb	0.73	0.02	0.03	190.4
HUPdb	0.29	0.04	0.02	314.5
FLCrw	0.44	0.16	0.44	7.3
FLCewb	0.97	0.02	0.12	41.4
FLClwb	0.76	0.02	0.14	36.2
FLCdb	0.21	0.09	0.20	22.0
AHArw	0.49	0.09	0.30	13.0
AHAewb	0.07	0.02	0.13	38.8
AHALwb	0.04	0.05	0.16	29.6
AHADb	0.02	0.10	0.11	43.8
DPPrw	0.48	0.11	0.33	11.7
DPPewb	0.89	0.02	0.12	41.9
DPPlwb	0.69	0.02	0.08	65.9
DPPdb	0.21	0.07	0.07	73.9

489

490

491 Table A1: Mean RW, EWB, LWB and DB values for the raw chronologies. Coefficient of variation (CV) and mean inter-series  
492 correlation (RBAR) are calculated from the 20-year spline detrended chronologies. n-EPS reflects the number of series needed to  
493 attain an EPS value of 0.85 related to the RBAR value (Wilson and Elling 2004).

TASMANIA

RCS - Celery Top

	RCSewb	RCSlwb	RCSdb
RCSrw	0.03	-0.64	0.67
RCSewb		0.22	0.27
RCSlwb			-0.82

MCK - Pencil Pine

	MCKewb	MCKlwb	MCKdb
MCKrw	-0.10	-0.41	0.45
MCKewb		0.57	-0.01
MCKlwb			-0.79

CM - Pencil Pine

	CMewb	CMlwb	CMdb
CMrw	0.01	-0.30	0.43
CMewb		0.68	-0.04
CMlwb			-0.71

MWWTRL - King Billy Pine

	MTewb	MTlwb	MTdb
MTrw	0.31	-0.40	0.62
MTewb		0.21	0.40
MTlwb			-0.76

MRD - King Billy Pine

	MRDewb	MRDlwb	MRDdb
MRDrw	0.18	-0.61	0.65
MRDewb		0.14	0.44
MRDlwb			-0.78

MHP - Huon Pine (high elevation)

	MHPewb	MHPlwb	MHPdb
MHPrw	0.64	-0.19	0.69
MHPewb		0.16	0.67
MHPlwb			-0.56

BUT - Huon Pine (low elevation)

	BUTewb	BUTlwb	BUTdb
BUTrw	-0.20	-0.49	0.31
BUTewb		0.21	0.35
BUTlwb			-0.72

NEW ZEALAND

PKL - Kauri

	PKLewb	PKLlwb	PKLdb
PKLrw	0.14	-0.37	0.54
PKLewb		0.44	0.42
PKLlwb			-0.55

HUP - Kauri

	HUPewb	HUPlwb	HUPdb
HUPrw	-0.02	-0.23	0.30
HUPewb		0.58	0.23
HUPlwb			-0.51

FLC - NZ Cedar

	FLCewb	FLClwb	FLCdb
FLCrw	0.40	-0.47	0.70
FLCewb		0.12	0.58
FLClwb			-0.66

AHA - Silver Pine

	AHAewb	AHAlwb	AHAdb
AHArw	0.12	-0.29	0.38
AHAewb		0.48	0.32
AHAlwb			-0.58

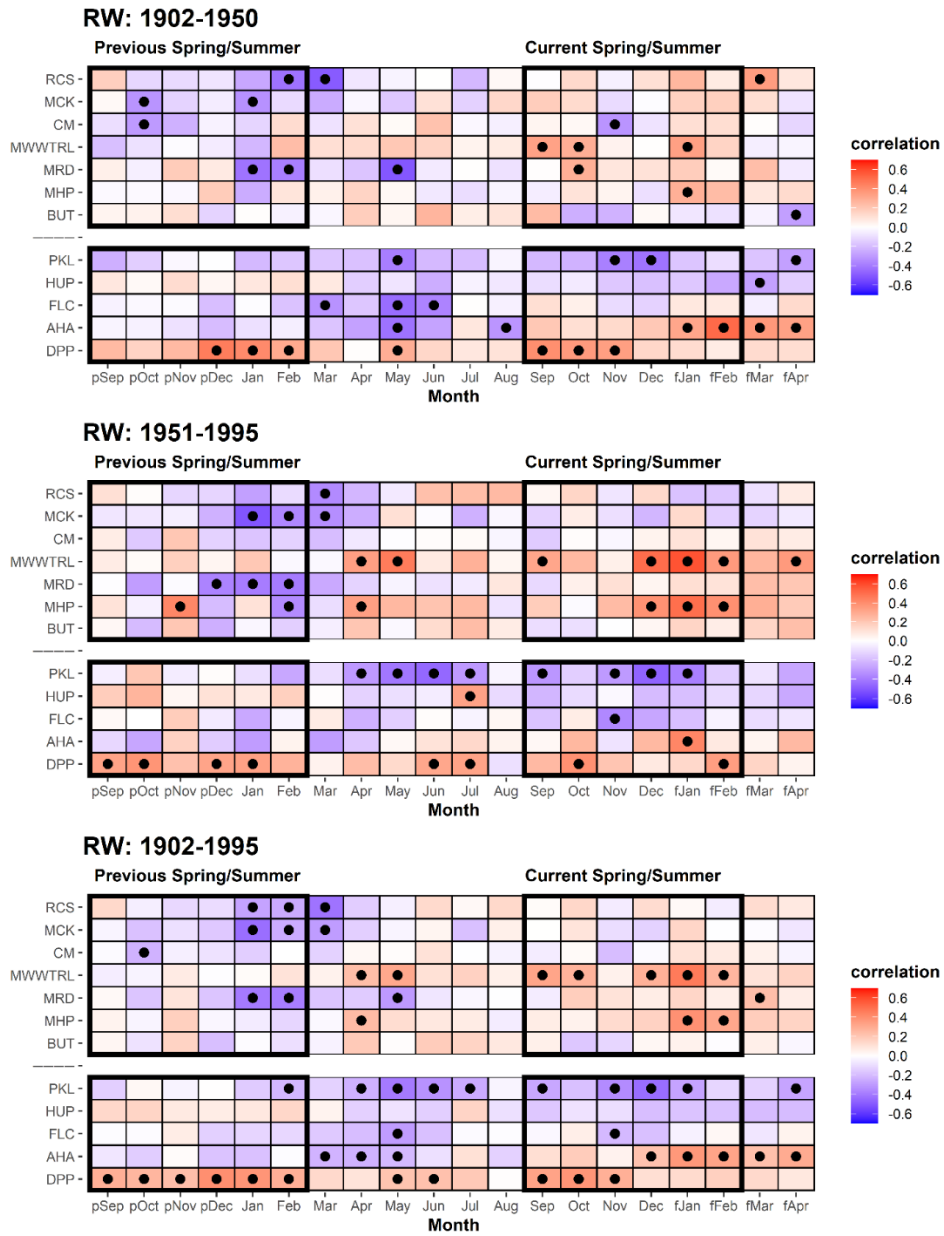
DPP - NZ Pink Pine

	DPPewb	DPPlwb	DPPdb
DPPrw	0.17	-0.25	0.51
DPPewb		0.60	0.60
DPPlwb			-0.20

494

495

496 Table A2: Correlation matrices for each site between the four detrended TR parameter chronologies (1798-1995). Grey shading  
497 denotes a significant correlation (95%).

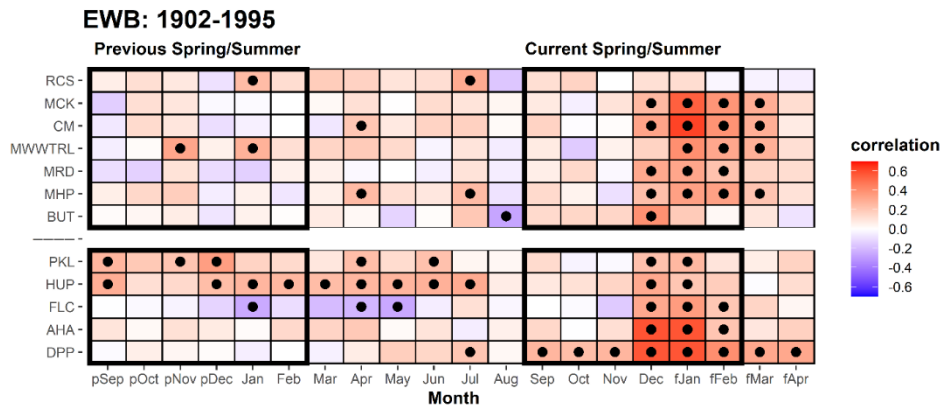
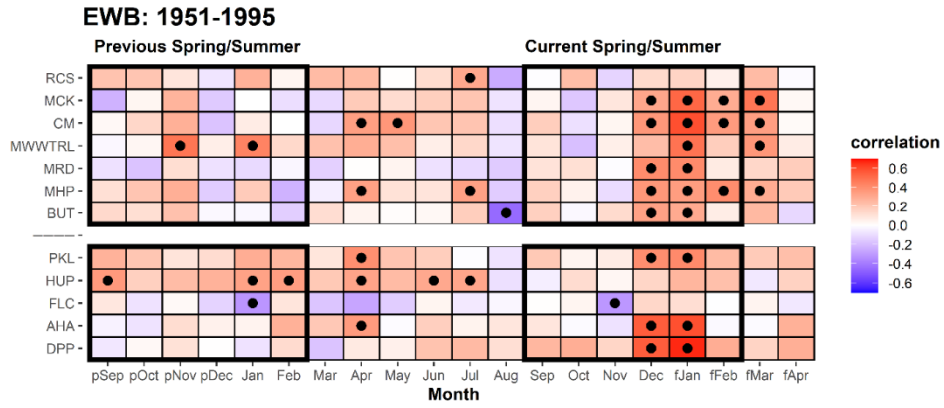
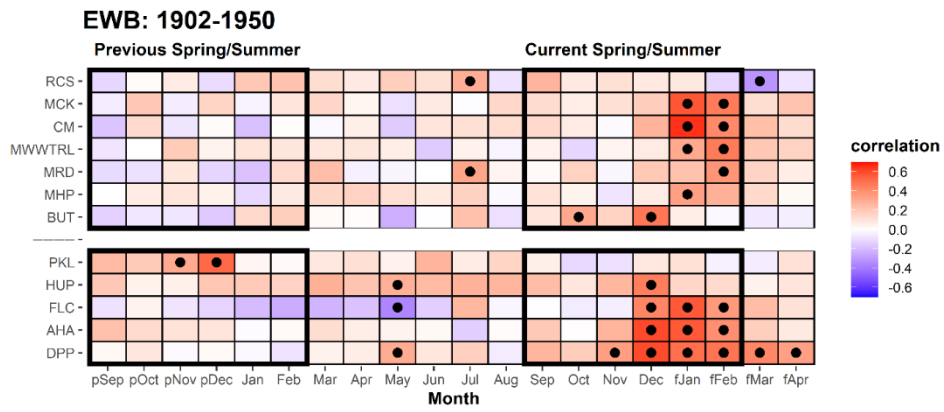


499

500

501 **Table A3a: Correlation response function analysis for ring-width with CRU TS temperatures. Analysis was undertaken over the**  
 502 **1902-1950, 1951-1995 and 1902-1995 periods. Black dots denoted correlations significant at the 95% C.L.**

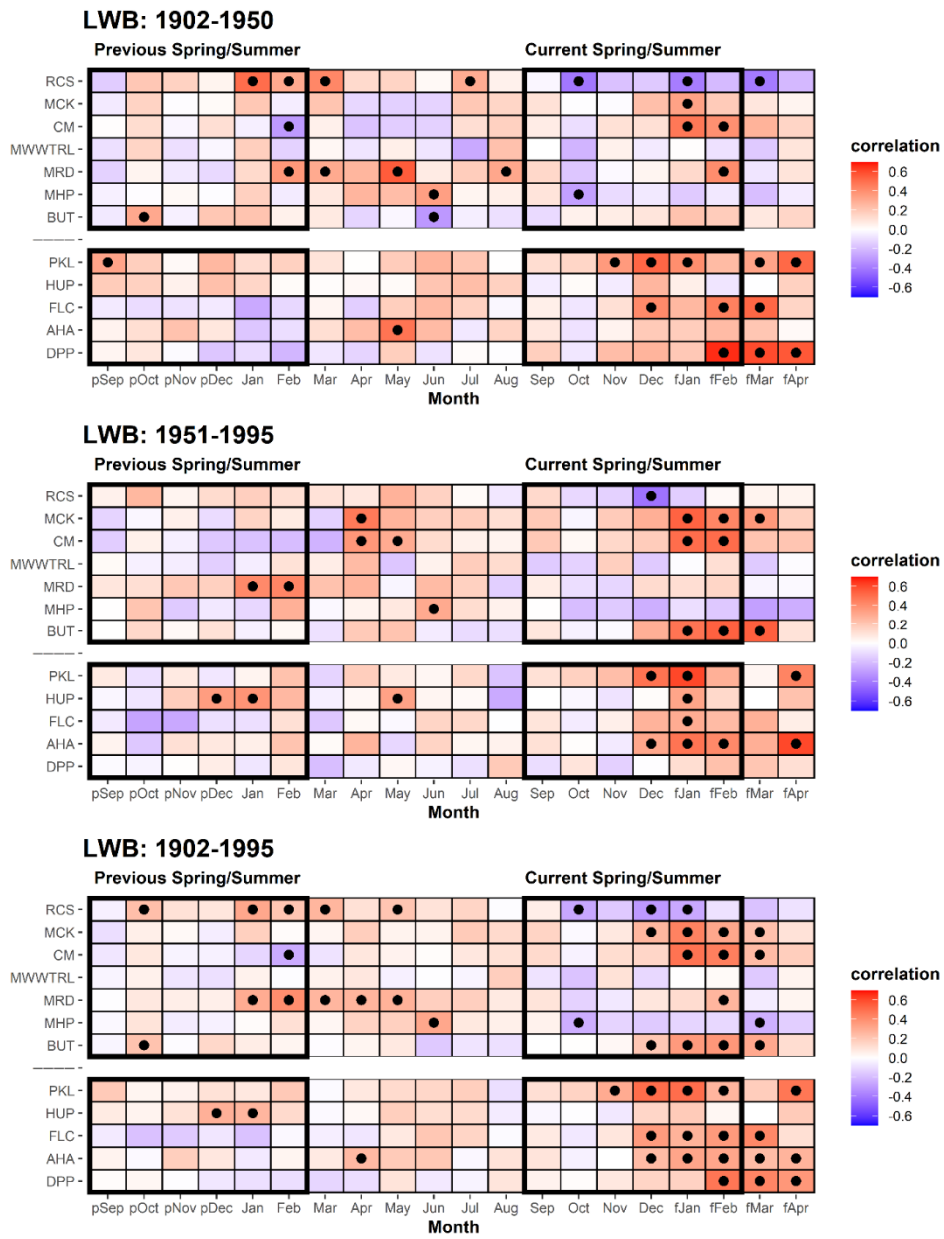
503



504

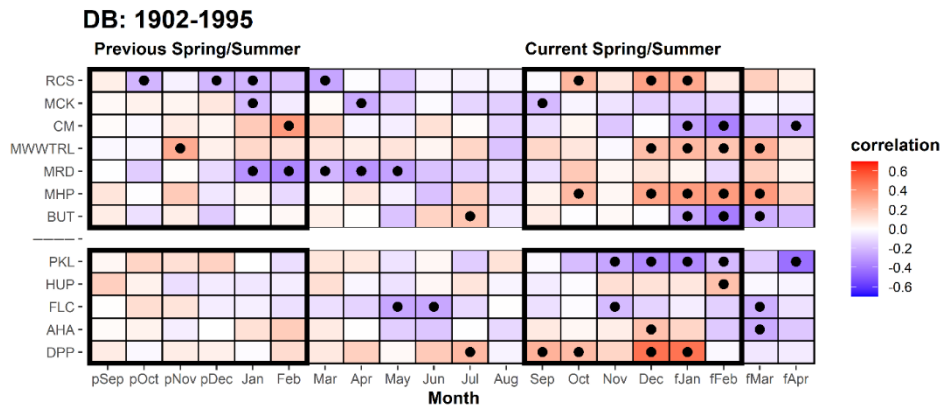
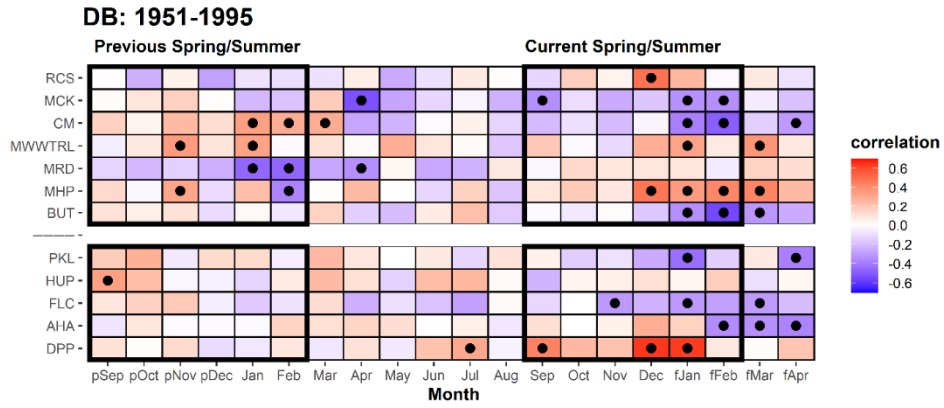
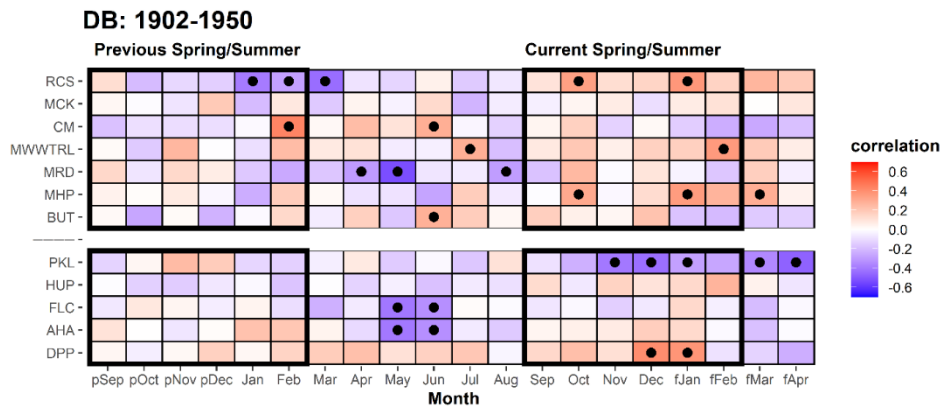
505 Table A3b: As 3a but for EWB.





506

507 Table A3c: As 3a but for LWB.

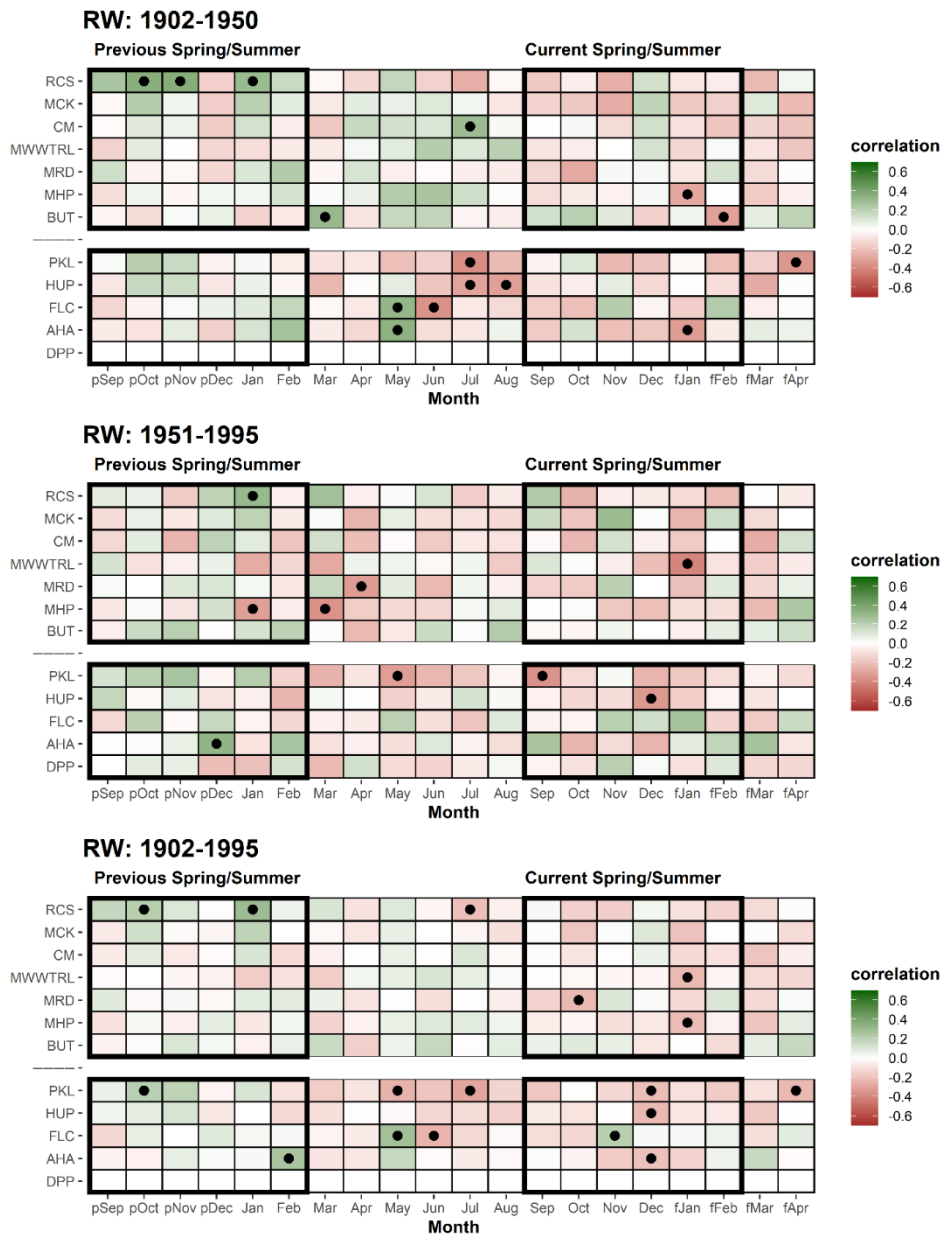


508

509 Table A3d: As 3a but for DB.

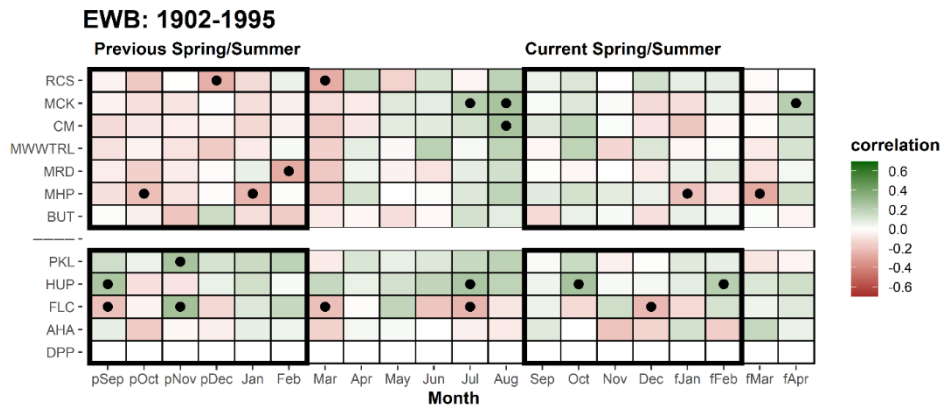
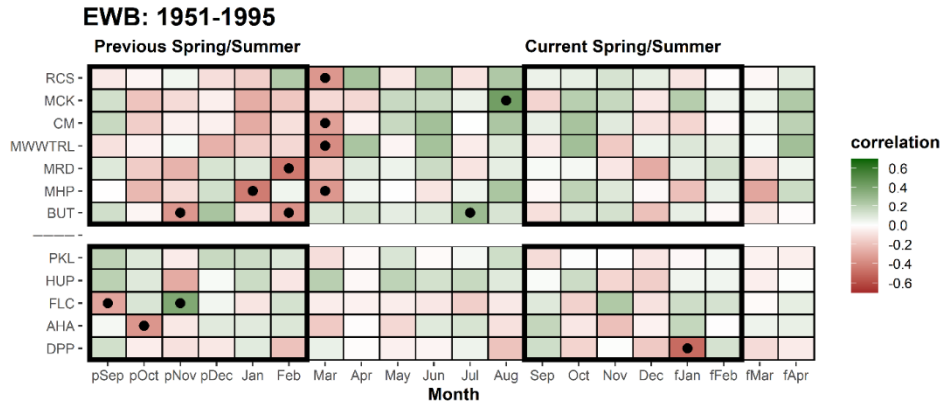
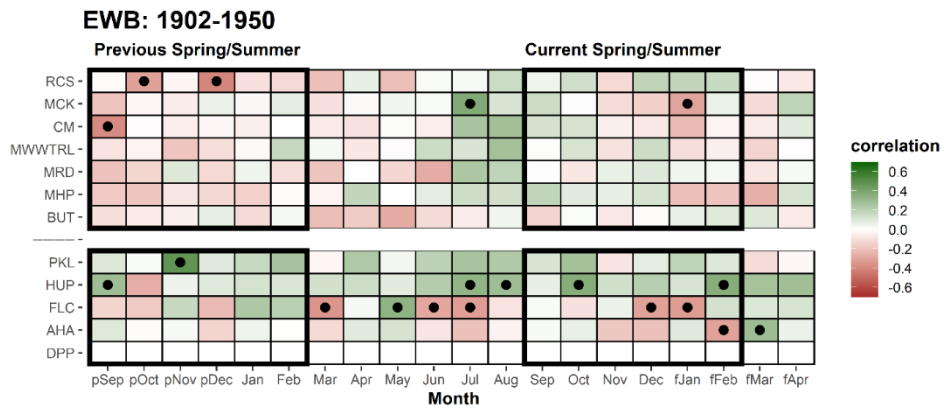
510

511



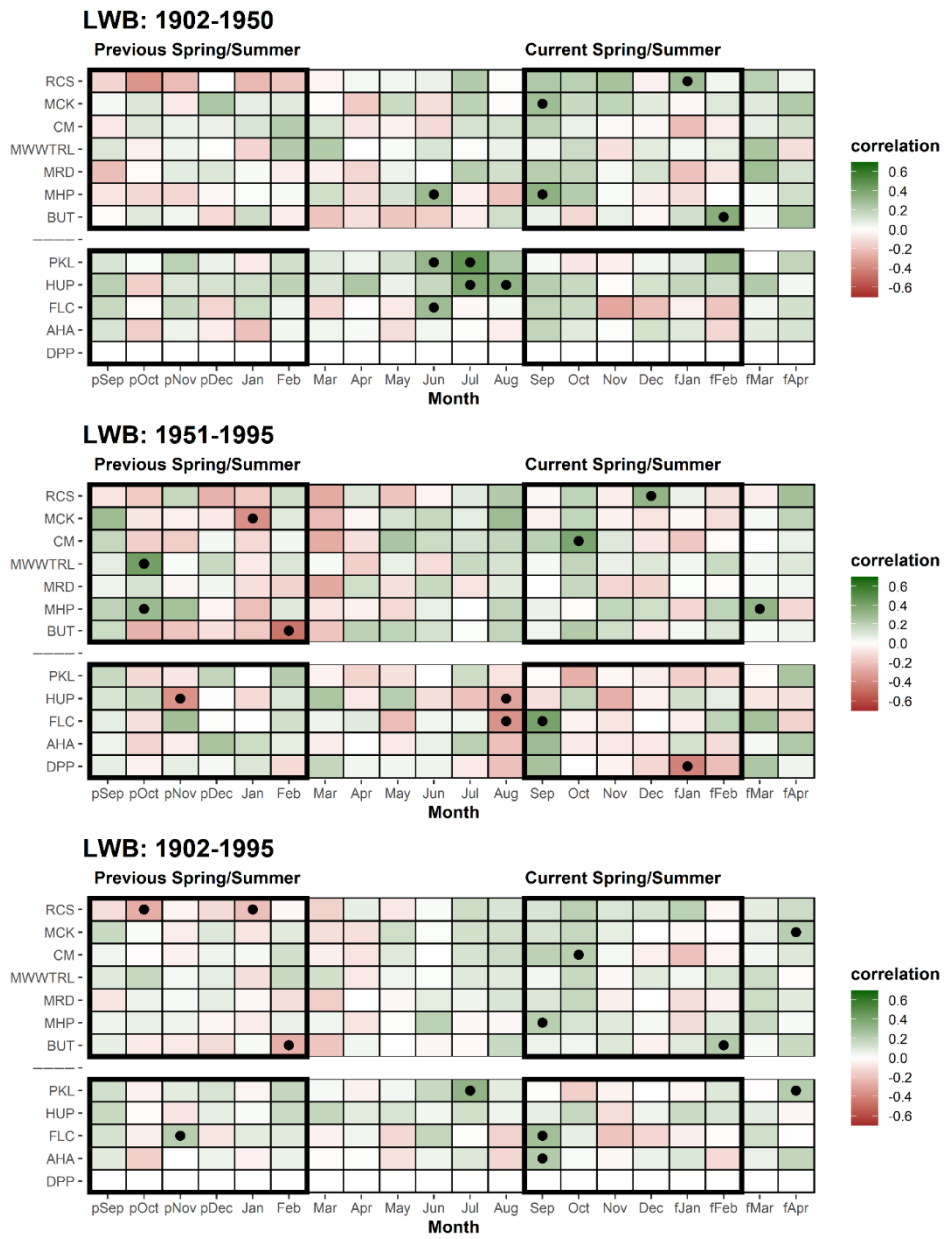
512

513 Table A4a: Correlation response function analysis for ring-width with CRU TS precipitation. Analysis was undertaken over the  
 514 1902-1950, 1951-1995 and 1902-1995 periods. Black dots denoted correlations significant at the 95% C.L.



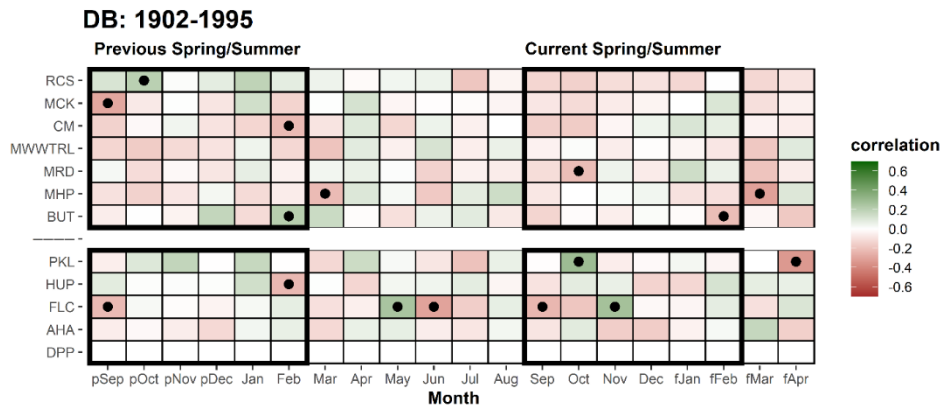
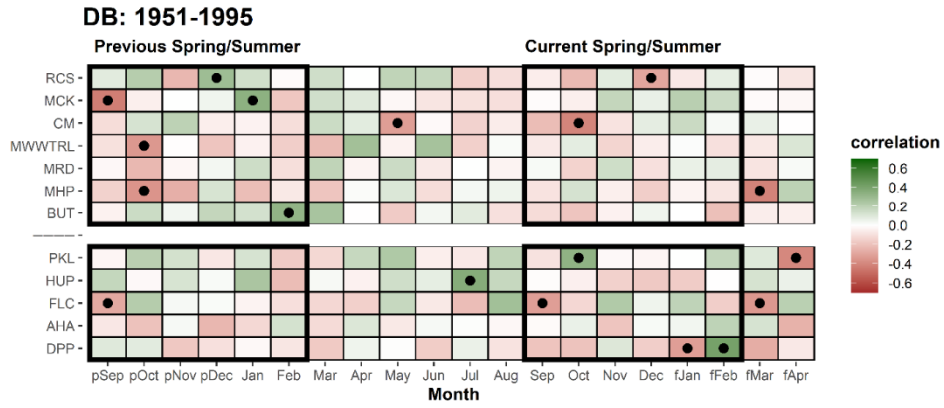
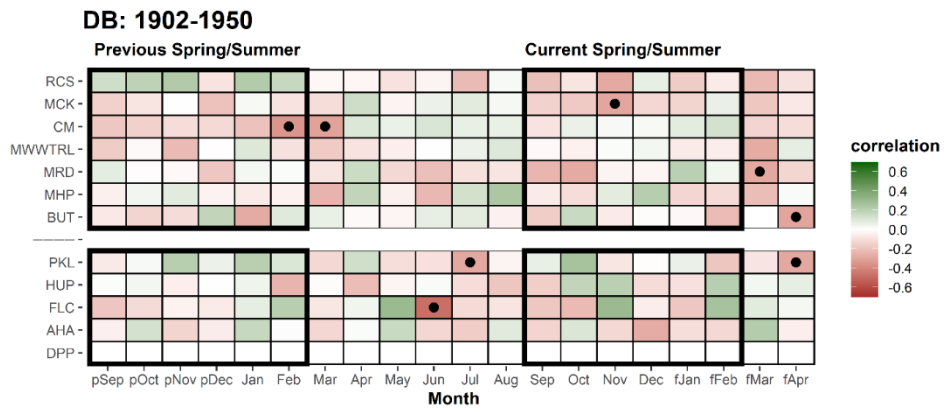
515

516 Table A4b: As 4a but for EWB.



517

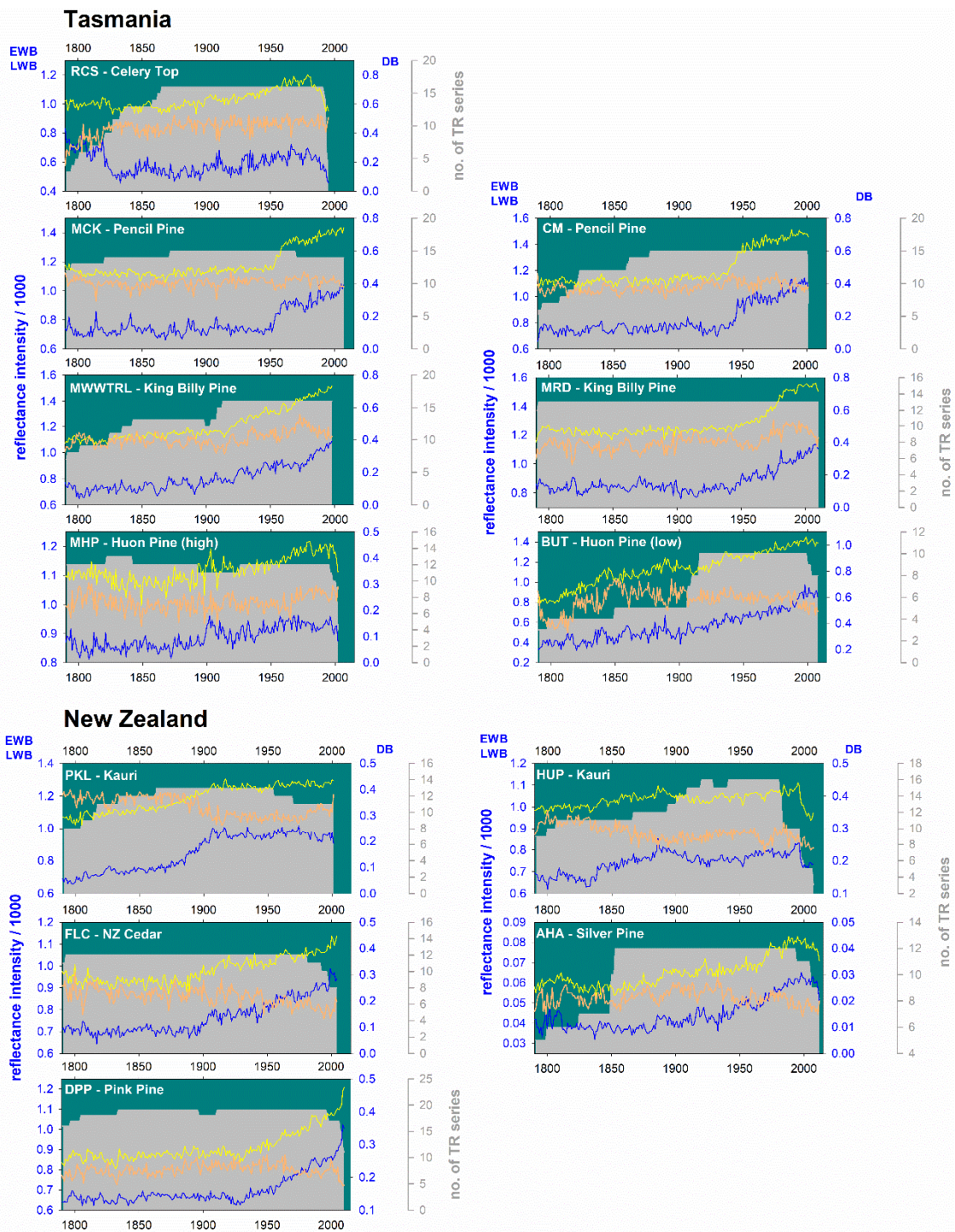
518 Table A4c: As 4a but for LWB.



519

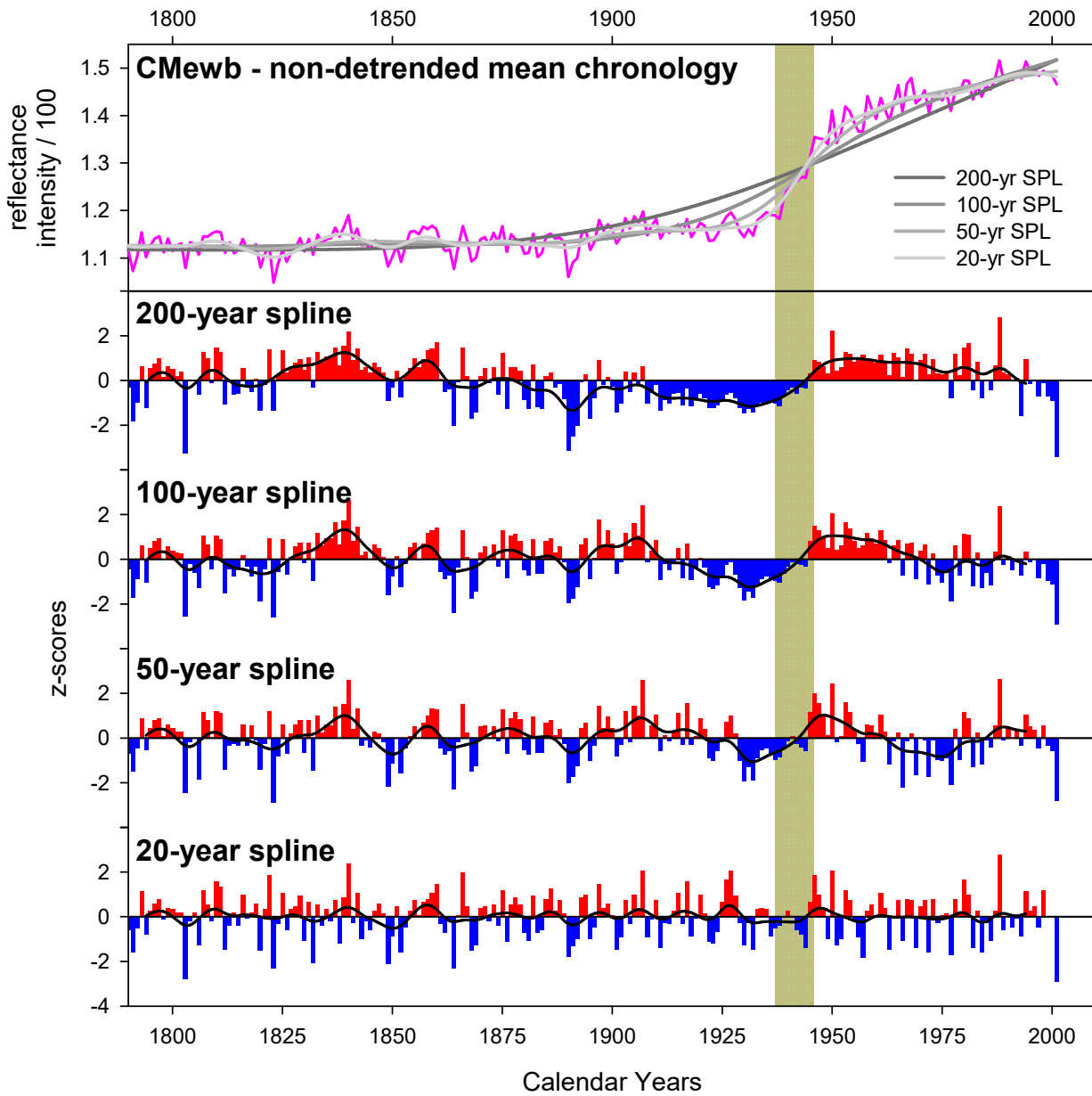
520 Table A4d: As 4a but for DB.

521



522

523 **Figure A1: Plots of raw mean chronologies of EWB (yellow), LWB (blue), DB (orange) and TR series replication (grey shading).**  
 524 **The left axis is for EWB and LWB, 1st right axis is DB, while 2nd right axis is series replication.**



526

527

528 **Figure A2: Upper panel: raw mean non-detrended EWB chronology for the CM Pencil Pine site. lower panel: represents**  
529 **progressively more flexible spline detrending options. The vertical grey bar denotes the heartwood/sapwood transition period.**

530



531

532

533

534 **6 Data availability**

535 All raw data will be archived at the International Tree-Ring Databank on acceptance of the manuscript

536

537 **7 Author contribution**

538 RW: Project conception

539 RW, KA, PB, SB, GB, BB, EC, RD, AF, PK, JP: Sample collection and image acquisition

540 RW, KA, SB, MG: Data generation

541 All: Paper writing, final methodological design, comment and editing

542 **8 Competing interests**

543 The authors declare that they have no conflict of interest

544 **9 Acknowledgements**

545 RW was funded through the University of Melbourne Dyason Fellowship in 2014 to undertake preliminary measurement and  
546 analyses for this study. We also acknowledge NSF-NERC funding (NE/W007223/1). Permission to obtain samples from the  
547 Tasmanian sites was provided by Parks and Wildlife Tasmania through several different permits over multiple years. KA  
548 was supported by the Australian Research Council grants DP1201040320 and LP12020811 to PB. Permissions to obtain  
549 samples from New Zealand and Tasmanian sites were provided over multiple years by the New Zealand Department of  
550 Conservation and Parks and Wildlife Tasmania.

551 **10 References**

552 Allen, K.J., Cook, E.R., Francey, R.J.. and Michael, K.: The climatic response of *Phyllocladus aspleniifolius* (Labill.) Hook.  
553 f in Tasmania. *Journal of Biogeography*, 28(3), pp.305-316. DOI: 10.1046/j.1365-2699.2001.00546.x. January 2002

554

555 Allen, K.J., Ogden, J., Buckley, B.M., Cook, E.R., and Baker, P.J.: The potential to reconstruct broadscale climate indices  
556 associated with southeast Australian droughts from *Athrotaxis* species, Tasmania. *Climate Dynamics*, 37(9-10), pp.1799-  
557 1821. DOI.org/10.1007/s00382-011-1011-7. February 2011  
558

559 Allen, K.J., Lee, G., Ling, F., Allie, S., Willis, M., and Baker, P.J.: Palaeohydrology in climatological context: developing  
560 the case for use of remote predictors in Australian streamflow reconstructions. *Applied Geography*, 64, pp.132-152. DOI:  
561 10.1016/j.apgeog.2015.09.007. October 2015a  
562

563 Allen, K.J., Nichols, S.C., Evans, R., Cook, E.R., Allie, S., Carson, G., Ling, F., and Baker, P.J.: Preliminary December-  
564 January inflow and streamflow reconstructions from tree rings for western Tasmania, southeastern Australia. *Water  
565 Resources Research*, 51(7), pp.5487-5503. DOI: 10.1002/2015WR017062. July 2015b  
566

567 Allen, K.J., Fenwick, P., Palmer, J.G., Nichols, S.C., Cook, E.R., Buckley, B.M., and Baker, P.J.: A 1700-year *Athrotaxis*  
568 *selaginoides* tree-ring width chronology from southeastern Australia. *Dendrochronologia*, 45, pp.90-100. DOI:  
569 10.1016/j.dendro.2017.07.004. July 2017  
570

571 Allen, K.J., Cook, E.R., Evans, R., Francey, R., Buckley, B.M., Palmer, J.G., Peterson, M.J. and Baker, P.J.: Lack of cool,  
572 not warm, extremes distinguishes late 20th Century climate in 979-year Tasmanian summer temperature reconstruction.  
573 *Environmental Research Letters*, 13(3), p.034041. DOI: 10.1088/1748-9326/aaafd7. February 2018  
574

575 Alexander, M.R., Pearl, J.K., Bishop, D.A., Cook, E.R., Anchukaitis, K.J. and Pederson, N.: The potential to strengthen  
576 temperature reconstructions in ecoregions with limited tree line using a multispecies approach. *Quaternary Research*, 92(2),  
577 pp.583-597. DOI: 10.1017/qua.2019.33. June 2019  
578

579 Altman, J.: Tree-ring-based disturbance reconstruction in interdisciplinary research: Current state and future directions.  
580 *Dendrochronologia*, p.125733. DOI: 10.1016/j.dendro.2020.125733. July 2020  
581

582 Arbelleay, E., Jarvis, I., Chavardès, R.D., Daniels, L.D. and Stoffel, M.: Tree-ring proxies of larch bud moth defoliation:  
583 latewood width and blue intensity are more precise than tree-ring width. *Tree Physiology* 38(8), 1237-1245. DOI:  
584 10.1093/treephys/tpy057. May 2018  
585

586 Babst, F., Poulter, B., Trouet, V., Tan, K., Neuwirth, B., Wilson, R., Carrer, M., Grabner, M., Tegel, W., Levanic, T. and  
587 Panayotov, M.: Site-and species-specific responses of forest growth to climate across the European continent. *Global  
588 Ecology and Biogeography*, 22(6), pp.706-717. DOI: 10.1111/geb.12023. June 2013

589

590 Babst, F., Wright, W.E., Szejner, P., Wells, L., Belmecheri, S., Monson, R.K.: Blue intensity parameters derived from  
591 Ponderosa pine tree rings characterize intra-annual density fluctuations and reveal seasonally divergent water limitations.  
592 *Trees* 30(4), 1403-1415. DOI: 10.1007/s00468-016-1377-6. August 2016

593

594 Björklund, J.A., Gunnarson, B.E., Seftigen, K., Esper, J., Linderholm, H.W.: Blue intensity and density from northern  
595 Fennoscandian tree rings, exploring the potential to improve summer temperature reconstructions with earlywood  
596 information. *Climate of the Past* 10(2), 877-885. DOI: 10.5194/cp-10-877-2014. April 2014a

597

598 Björklund, J., Gunnarson, B.E., Seftigen, K., Zhang, P., Linderholm, H.W.: Using adjusted blue intensity data to attain high-  
599 quality summer temperature information: a case study from Central Scandinavia. *The Holocene* 25(3), 547-556. DOI:  
600 10.1177/0959683614562434. February 2014b

601

602 Björklund, J., Seftigen, K., Schweingruber, F., Fonti, P., von Arx, G., Bryukhanova, M.V., Cuny, H.E., Carrer, M.,  
603 Castagneri, D. and Frank, D.C.: Cell size and wall dimensions drive distinct variability of earlywood and latewood density in  
604 Northern Hemisphere conifers. *New Phytologist*, 216(3), pp.728-740. DOI.org/10.1111/nph.14639. June 2017

605

606 Björklund, J., von Arx, G., Nievergelt, D., Wilson, R., Van den Bulcke, J., Günther, B., Loader, N.J., Rydval, M., Fonti, P.,  
607 Scharnweber, T. and Andreu-Hayles, L. et al.: Scientific merits and analytical challenges of tree-ring densitometry. *Reviews*  
608 *of Geophysics*, 57(4), pp.1224-1264. DOI: 10.1029/2019RG000642. October 2019

609

610 Björklund, J., Seftigen, K., Fonti, P., Nievergelt, D., von Arx, G.: Dendroclimatic potential of dendroanatomy in  
611 temperature-sensitive *Pinus sylvestris*. *Dendrochronologia* 60, 125673. DOI: 10.1016/j.dendro.2020.125673. February 2020.

612

613 Blake, S.A., Palmer, J.G., Björklund, J., Harper, J.B. and Turney, C.S.: Palaeoclimate potential of New Zealand *Manoao*  
614 *colensoi* (silver pine) tree rings using Blue-Intensity (BI). *Dendrochronologia*, 60, p.125664. DOI:  
615 10.1016/j.dendro.2020.125664. April 2020

616

617 Boswijk, G., Fowler, A.M., Palmer, J.G., Fenwick, P., Hogg, A., Lorrey, A. and Wunder, J.: The late Holocene kauri  
618 chronology: assessing the potential of a 4500-year record for palaeoclimate reconstruction. *Quaternary Science Reviews*, 90,  
619 pp.128-142. DOI: 10.1016/j.quascirev.2014.02.022. April 2014

620

621 Bradley, R.S.: *Paleoclimatology: reconstructing climates of the Quaternary*. Elsevier. 1999

622

623 Briffa, K.R., Osborn, T.J., Schweingruber, F.H., Jones, P.D., Shiyatov, S.G. and Vaganov, E.A.: Tree-ring width and density  
624 data around the Northern Hemisphere: Part 1, local and regional climate signals. *The Holocene*, 12(6), pp.737-757. DOI:  
625 10.1191/0959683602hl587rp. November 2002  
626  
627 Brookhouse, M. and Graham, R.: Application of the minimum blue-intensity technique to a southern-hemisphere conifer.  
628 *Tree-Ring Research*, 72(2), pp.103-107. DOI: 10.3959/1536-1098-72.02.103. July 2016  
629  
630 Buckley, B.M., Cook, E.R., Peterson, M.J. and Barbetti, M.: A changing temperature response with elevation for  
631 *Lagarostrobos franklinii* in Tasmania, Australia. In *Climatic Change at High Elevation Sites* (pp. 245-266). Springer,  
632 Dordrecht. DOI: 10.1023/A:1005322332230. January 1997  
633  
634 Buckley, B., Ogden, J., Palmer, J., Fowler, A. and Salinger, J.: Dendroclimatic interpretation of tree-rings in *Agathis*  
635 *australis* (kauri). 1. Climate correlation functions and master chronology. *Journal of the Royal Society of New Zealand*,  
636 30(3), pp.263-276. DOI: 10.1080/10412905.2002.9699839. September 2000  
637  
638 Buckley, B.M., Hansen, K.G., Griffin, K.L., Schmiege, S., Oelkers, R., D'Arrigo, R.D., Stahle, D.K., Davi, N., Nguyen,  
639 T.Q.T., Le, C.N. and Wilson, R.J.: Blue intensity from a tropical conifer's annual rings for climate reconstruction: An  
640 ecophysiological perspective. *Dendrochronologia*, 50, pp.10-22. DOI: 10.1016/j.dendro.2018.04.003. April 2018  
641  
642 Büntgen, U., Krusic, P.J., Verstege, A., Sangüesa-Barreda, G., Wagner, S., Camarero, J.J., Ljungqvist, F.C., Zorita, E.,  
643 Oppenheimer, C., Konter, O. and Tegel, W.: New tree-ring evidence from the Pyrenees reveals Western Mediterranean  
644 climate variability since medieval times. *Journal of Climate*, 30(14), pp.5295-5318. DOI: 10.1175/JCLI-D-16-0526.1. March  
645 2017  
646  
647 Büntgen, U., Urban, O., Krusic, P.J., Rybníček, M., Kolář, T., Kyncl, T., Ač, A., Koňasová, E., Čáslavský, J., Esper, J. and  
648 Wagner, S.: Recent European drought extremes beyond Common Era background variability. *Nature Geoscience*, 14(4),  
649 pp.190-196. DOI: 10.1038/s41561-021-00698-0. April 2021  
650  
651 Buras, A.: A comment on the expressed population signal. *Dendrochronologia*, 44, pp.130-132. DOI:  
652 10.1016/j.dendro.2017.03.005. May 2017  
653  
654 Buras, A., Spyt, B., Janecka, K., Kaczka, R.: Divergent growth of Norway spruce on Babia Góra Mountain in the western  
655 Carpathians. *Dendrochronologia* 50, 33-43. DOI: 10.1016/j.dendro.2018.04.005. April 2018  
656

657 Camarero, J.J., Rozas, V. and Olano, J.M.: Minimum wood density of *Juniperus thurifera* is a robust proxy of spring water  
658 availability in a continental Mediterranean climate. *Journal of Biogeography*, 41(6), pp.1105-1114. DOI: 10.1111/jbi.12271.  
659 February 2014  
660

661 Camarero, J.J., Fernández-Pérez, L., Kirilyanov, A.V., Shestakova, T.A., Knorre, A.A., Kukarskih, V.V. and Voltas, J.:  
662 Minimum wood density of conifers portrays changes in early season precipitation at dry and cold Eurasian regions. *Trees*,  
663 31(5), pp.1423-1437. DOI: 10.1007/s00468-017-1559-x. October 2017  
664

665 Campbell, R., McCarroll, D., Loader, N.J., Grudd, H., Robertson, I., Jalkanen, R.: Blue intensity in *Pinus sylvestris* tree-  
666 rings: developing a new palaeoclimate proxy. *The Holocene* 17(6), 821-828. DOI: 10.1177/0959683607080523. September  
667 2007  
668

669 Campbell, R., McCarroll, D., Robertson, I., Loader, N.J., Grudd, H., Gunnarson, B.: Blue intensity in *Pinus sylvestris* tree  
670 rings: a manual for a new palaeoclimate proxy. *Tree-Ring Research* 67(2), 127-135. DOI: 10.3959/2010-13.1. July 2011  
671

672 Cleaveland, M.K.: Climatic response of densitometric properties in semiarid site tree rings. *Tree-Ring Bull* 46:13–29. 1986  
673

674 Cook, E.R. and Peters, K.: The smoothing spline: a new approach to standardizing forest interior tree-ring width series for  
675 dendroclimatic studies. 1981  
676

677 Cook, E. R.: The Decomposition of Tree-Ring Series for Environmental Studies. *Tree-Ring Bulletin* 47: 37–59. 1987  
678

679 Cook, E.R., Briffa, K.R. and Jones, P.D.: Spatial regression methods in dendroclimatology: a review and comparison of two  
680 techniques. *International Journal of Climatology*, 14(4), pp.379-402. doi.org/10.1002/joc.3370140404. 1994  
681

682 Cook, E.R., Palmer, J.G., Cook, B.I., Hogg, A. and D'Arrigo, R.: A multi-millennial palaeoclimatic resource from  
683 *Lagarostrobos colensoi* tree-rings at Oroko Swamp, New Zealand. *Global and Planetary Change*, 33(3-4), pp.209-220. DOI:  
684 10.1016/S0921-8181(02)00078-4. July 2002  
685

686 Cook, E.R., Buckley, B.M., Palmer, J.G., Fenwick, P., Peterson, M.J., Boswijk, G. and Fowler, A.: Millennia-long tree-ring  
687 records from Tasmania and New Zealand: A basis for modelling climate variability and forcing, past, present and future.  
688 *Journal of Quaternary Science: Published for the Quaternary Research Association*, 21(7), pp.689-699. DOI:  
689 10.1002/jqs.1071. October 2006  
690

691 Cook, E.R. and Pederson, N.: Uncertainty, emergence, and statistics in dendrochronology. In *Dendroclimatology* (pp. 77-  
692 112). Springer, Dordrecht. DOI: 10.1007/978-1-4020-5725-0\_4. September 2011  
693

694 D'Arrigo, R.D., Buckley, B.M., Cook, E.R. and Wagner, W.S.: Temperature-sensitive tree-ring width chronologies of pink  
695 pine (*Halocarpus biformis*) from Stewart Island, New Zealand. *Palaeogeography, Palaeoclimatology, Palaeoecology*, 119(3-  
696 4), pp.293-300. DOI:10.1016/0031-0182(95)00014-3. 1996  
697

698 Davi, N.K., Rao, M.P., Wilson, R., Andreu-Hayles, L., Oelkers, R., D'Arrigo, R., Nachin, B., Buckley, B., Pederson, N.,  
699 Leland, C. and Suran, B.: Accelerated Recent Warming and Temperature Variability over the Past Eight Centuries in the  
700 Central Asian Altai from Blue Intensity in Tree Rings. *Geophysical Research Letters*. doi.org/10.1029/2021GL092933. July  
701 2021  
702

703 Dolgova, E.: June–September temperature reconstruction in the Northern Caucasus based on blue intensity data.  
704 *Dendrochronologia* 39, 17-23. DOI: 10.1016/j.dendro.2016.03.002. March 2016  
705

706 Drew, D.M., Allen, K., Downes, G.M., Evans, R., Battaglia, M. and Baker, P.: Wood properties in a long-lived conifer  
707 reveal strong climate signals where ring-width series do not. *Tree Physiology*, 33(1), pp.37-47. DOI:  
708 10.1093/treephys/tps111. November 2012  
709

710 Druckenbrod, D.L., Pederson, N., Rentch, J. and Cook, E.R.: A comparison of times series approaches for dendroecological  
711 reconstructions of past canopy disturbance events. *Forest ecology and management*, 302, pp.23-33. DOI:  
712 10.1016/j.foreco.2013.03.040. April 2013  
713

714 Duncan, R.P., Fenwick, P., Palmer, J.G., McGlone, M.S. and Turney, C.S.: Non-uniform interhemispheric temperature  
715 trends over the past 550 years. *Climate Dynamics*, 35(7-8), pp.1429-1438. DOI: 10.1007/s00382-010-0794-2. December  
716 2010  
717

718 Esper, J., Frank, D.C., Timonen, M., Zorita, E., Wilson, R.J., Luterbacher, J., Holzkämper, S., Fischer, N., Wagner, S.,  
719 Nievergelt, D. and Verstege, A.: Orbital forcing of tree-ring data. *Nature Climate Change*, 2(12), pp.862-866. DOI:  
720 10.1038/NCLIMATE1589. July 2012  
721

722 Evans R.: Rapid measurement of the transverse dimensions of tracheids in radial wood sections from *Pinus radiata*.  
723 *Holzforschung* 48: 168–172. doi.org/10.1515/hfsg.1994.48.2.168. 1994  
724

725 Fonti, P., Bryukhanova, M.V., Myglan, V.S., Kirilyanov, A.V., Naumova, O.V. and Vaganov, E.A.: Temperature-induced  
726 responses of xylem structure of *Larix sibirica* (Pinaceae) from the Russian Altay. *American journal of botany*, 100(7),  
727 pp.1332-1343. DOI: 10.3732/ajb.1200484. May 2013  
728

729 Fowler, A., Palmer, J., Salinger, J. and Ogden, J.: Dendroclimatic interpretation of tree-rings in *Agathis australis* (kauri): 2.  
730 Evidence of a significant relationship with ENSO. *Journal of the Royal Society of New Zealand*, 30(3), pp.277-292. DOI:  
731 10.1080/03014223.2000.9517622. September 2000  
732

733 Fowler, A.M., Boswijk, G., Lorrey, A.M., Gergis, J., Pirie, M., McCloskey, S.P., Palmer, J.G. and Wunder, J.: Multi-  
734 centennial tree-ring record of ENSO-related activity in New Zealand. *Nature Climate Change*, 2(3), pp.172-176. DOI:  
735 10.1038/nclimate1374. March 2012  
736

737 Fritts, H.C., Smith, D.G., Cardis, J.W. and Budelsky, C.A.: Tree-ring characteristics along a vegetation gradient in northern  
738 Arizona. *Ecology*, 46(4), pp.393-401. doi.org/10.2307/1934872. 1965  
739

740 Fritts, H.C.: *Tree Rings and Climate*. London: Academic Press Ltd. 1976  
741

742 Fuentes, M., Salo, R., Björklund, J., Seftigen, K., Zhang, P., Gunnarson, B., Aravena, J.C., Linderholm, H.W.: A 970-year-  
743 long summer temperature reconstruction from Roggen, west-central Sweden, based on blue intensity from tree rings. *The*  
744 *Holocene* 28(2), 254-266. DOI: 10.1177/0959683617721322. August 2017  
745

746 Harley, G.L., Heeter, K.J., Maxwell, J.T., Rayback, S.A., Maxwell, R.S., Reinemann, T.E. and H Taylor, A.: Towards broad-  
747 scale temperature reconstructions for Eastern North America using blue light intensity from tree rings. *International Journal*  
748 *of Climatology* 41:S1. DOI: 10.1002/joc.6910. January 2021  
749

750 Harris, I.P.D.J., Jones, P.D., Osborn, T.J. and Lister, D.H.: Updated high-resolution grids of monthly climatic observations–  
751 the CRU TS3. 10 Dataset. *International journal of climatology*, 34(3), pp.623-642. DOI: 10.1002/joc.3711. March 2014  
752

753 Heeter, K.J., Harley, G.L., Maxwell, J.T., McGee, J.H. and Matheus, T.J.: Late summer temperature variability for the  
754 Southern Rocky Mountains (USA) since 1735 CE: applying blue light intensity to low-latitude *Picea engelmannii* Parry ex  
755 Engelm. *Climatic Change*, 162(2), pp.965-988. DOI: 10.1007/s10584-020-02772-9. September 2020  
756

757 Helama, S., Arentoft, B.W., Collin-Haubensak, O., Hyslop, M.D., Brandstrup, C.K., Mäkelä, H.M., Tian, Q. Wilson, R.:  
758 Dendroclimatic signals deduced from riparian versus upland forest interior pines in North Karelia, Finland. *Ecological*  
759 *Research* 28(6), 1019-1028. DOI: 10.1007/s11284-013-1084-3. September 2013  
760  
761 Kaczka, R.J., Spyt, B., Janecka, K., Beil, I., Büntgen, U., Scharnweber, T., Nievergelt, D., Wilmking, M.: Different  
762 maximum latewood density and blue intensity measurements techniques reveal similar results. *Dendrochronologia* 49, 94-  
763 101. DOI: 10.1016/j.dendro.2018.03.005. March 2018  
764  
765 Kaczka, R.J. and Wilson, R.: I-BIND: International Blue Intensity Network Development Working Group.  
766 *Dendrochronologia*. DOI: 10.1016/j.dendro.2021.125859. June 2021  
767  
768 Kienast, F., Schweingruber, F.H., Bräker, O.U. and Schär, E., 1987. Tree-ring studies on conifers along ecological gradients  
769 and the potential of single-year analyses. *Canadian Journal of Forest Research*, 17(7), pp.683-696. DOI: 10.1139/x87-111.  
770 February 2011  
771  
772 Ljungqvist, F.C., Thejll, P., Björklund, J., Gunnarson, B.E., Piermattei, A., Rydval, M., Seftigen, K., Støve, B. and Büntgen,  
773 U.: Assessing non-linearity in European temperature-sensitive tree-ring data. *Dendrochronologia*, 59, p.125652. DOI:  
774 10.1016/j.dendro.2019.125652. November 2019  
775  
776 Loader, N.J., Santillo, P.M., Woodman-Ralph, J.P., Rolfe, J.E., Hall, M.A., Gagen, M., Robertson, I., Wilson, R., Froyd,  
777 C.A. and McCarroll, D.: Multiple stable isotopes from oak trees in southwestern Scotland and the potential for stable isotope  
778 dendroclimatology in maritime climatic regions. *Chemical Geology*, 252(1-2), pp.62-71. DOI:  
779 10.1016/j.chemgeo.2008.01.006. June 2008  
780  
781 Loader, N.J., Young, G.H., McCarroll, D., Davies, D., Miles, D. and Bronk Ramsey, C.: Summer precipitation for the  
782 England and Wales region, 1201–2000 CE, from stable oxygen isotopes in oak tree rings. *Journal of Quaternary Science*.  
783 DOI: 10.1002/jqs.3226. June 2020  
784  
785 Lorimer, C.G. and Frelich, L.E.: A methodology for estimating canopy disturbance frequency and intensity in dense  
786 temperate forests. *Canadian Journal of Forest Research*, 19(5), pp.651-663. DOI: 10.1139/x89-102. May 1989  
787  
788 McCarroll, D., Pettigrew, E., Luckman, A., Guibal, F. and Edouard, J.L.: Blue reflectance provides a surrogate for latewood  
789 density of high-latitude pine tree rings. *Arctic, Antarctic, and Alpine Research*, 34(4), pp.450-453. DOI: 10.2307/1552203.  
790 November 2002



791

792 McCarroll, D. and Loader, N.J.: Stable isotopes in tree rings. *Quaternary Science Reviews*, 23(7-8), pp.771-801. DOI:  
793 10.1016/j.quascirev.2003.06.017. April 2004

794

795 Neukom, R., Gergis, J., Karoly, D.J., Wanner, H., Curran, M., Elbert, J., González-Rouco, F., Linsley, B.K., Moy, A.D.,  
796 Mundo, I. and Raible, C.C.: Inter-hemispheric temperature variability over the past millennium. *Nature Climate Change*,  
797 4(5), pp.362-367. DOI: 10.1038/nclimate2174. March 2014

798

799 O'Donnell, A.J., Allen, K.J., Evans, R.M., Cook, E.R., Trouet, V. and Baker, P.J.: Wood density provides new opportunities  
800 for reconstructing past temperature variability from southeastern Australian trees. *Global and Planetary Change*, 141, pp.1-  
801 11. DOI: 10.1016/j.gloplacha.2016.03.010. April 2016

802

803 Palmer, J.G. and Xiong, L.: New Zealand climate over the last 500 years reconstructed from *Libocedrus bidwillii* Hook. f.  
804 tree-ring chronologies. *The Holocene*, 14(2), pp.282-289. DOI: 10.1191/0959683604hl679rr. March 2004

805

806 Panyushkina, I.P., Hughes, M.K., Vaganov, E.A. and Munro, M.A.: Summer temperature in northeastern Siberia since 1642  
807 reconstructed from tracheid dimensions and cell numbers of *Larix cajanderi*. *Canadian Journal of Forest Research*, 33(10),  
808 pp.1905-1914. DOI: 10.1139/x03-109. October 2003

809

810 Prendin, A.L., Petit, G., Carrer, M., Fonti, P., Björklund, J. and von Arx, G.: New research perspectives from a novel  
811 approach to quantify tracheid wall thickness. *Tree Physiology*, 37(7), pp.976-983. DOI: 10.1093/treephys/tpx037. April 2017

812

813 Reid, E. and Wilson, R.: Delta Blue Intensity vs. Maximum Density: A Case Study using *Pinus uncinata* in the Pyrenees.  
814 *Dendrochronologia*. DOI: 10.1016/j.dendro.2020.125706. May 2020

815

816 Rohde, R., Muller, R.A., Jacobsen, R., Muller, E., Perlmutter, S., Rosenfeld, A., Wurtele J., Groom D., and Wickham C. A  
817 new estimate of the average earth surface land temperature spanning 1753 to 2011. *Geoinformatics & Geostatistics: An*  
818 *Overview 1*: 1. Doi: 10.4172/2327-4581.1000101. January 2013

819

820 Rydval, M., Larsson, L.Å., McGlynn, L., Gunnarson, B.E., Loader, N.J., Young, G.H., Wilson, R.: Blue intensity for  
821 dendroclimatology: should we have the blues? Experiments from Scotland. *Dendrochronologia* 32(3), 191-204. DOI:  
822 10.1016/j.dendro.2014.04.003. December 2014

823

824 Rydval, M., Druckenbrod, D., Anchukaitis, K.J. and Wilson, R.: Detection and removal of disturbance trends in tree-ring  
825 series for dendroclimatology. *Canadian Journal of Forest Research*, 46(3), pp.387-401. DOI: 10.1139/cjfr-2015-0366.  
826 December 2015  
827

828 Rydval, M., Loader, N.J., Gunnarson, B.E., Druckenbrod, D.L., Linderholm, H.W., Moreton, S.G., Wood, C.V. and Wilson,  
829 R.: Reconstructing 800 years of summer temperatures in Scotland from tree rings. *Climate Dynamics*, 49(9-10), pp.2951-  
830 2974. DOI: 10.1007/s00382-016-3478-8. November 2017  
831

832 Rydval, M., Druckenbrod, D.L., Svoboda, M., Trotsiuk, V., Janda, P., Mikoláš, M., Čada, V., Bače, R., Teodosiu, M.,  
833 Wilson, R.: Influence of sampling and disturbance history on climatic sensitivity of temperature-limited conifers. *The*  
834 *Holocene* 28(10), 1574-1587. DOI: 10.1177/0959683618782605. July 2018  
835

836 Seftigen, K., Fuentes, M., Ljungqvist, F.C. and Björklund, J.: Using Blue Intensity from drought-sensitive *Pinus sylvestris* in  
837 Fennoscandia to improve reconstruction of past hydroclimate variability. *Climate Dynamics*, pp.1-16. DOI: 10.1007/s00382-  
838 020-05287-2. August 2020  
839

840 St. George, S.: An overview of tree-ring width records across the Northern Hemisphere. *Quaternary Science Reviews*, 95,  
841 pp.132-150. DOI: 10.1016/j.quascirev.2014.04.029. July 2014  
842

843 Trotsiuk, V., Pederson, N., Druckenbrod, D.L., Orwig, D.A., Bishop, D.A., Barker-Plotkin, A., Fraver, S. and Martin-Benito,  
844 D.: Testing the efficacy of tree-ring methods for detecting past disturbances. *Forest Ecology and Management*, 425, pp.59-  
845 67. DOI: 10.1016/j.foreco.2018.05.045. October 2018  
846

847 Visser, H. and Molenaar, J.: Kalman filter analysis in dendroclimatology. *Biometrics*, pp.929-940. DOI: 10.2307/2531724.  
848 December 1988  
849

850 von Arx, G., Crivellaro, A., Prendin, A.L., Čufar, K. and Carrer, M.: Quantitative wood anatomy—practical guidelines.  
851 *Frontiers in plant science*, 7, p.781. DOI: 10.3389/fpls.2016.00781. June 2016  
852

853 Wang, L., Payette, S. and Bégin, Y.: Relationships between anatomical and densitometric characteristics of black spruce and  
854 summer temperature at tree line in northern Quebec. *Canadian Journal of Forest Research*, 32(3), pp.477-486. DOI:  
855 10.1139/x01-208. March 2002  
856

857 Wigley, T.M., Briffa, K.R. and Jones, P.D.: On the average value of correlated time series, with applications in  
858 dendroclimatology and hydrometeorology. *Journal of Applied Meteorology and Climatology*, 23(2), pp.201-213.  
859 doi.org/10.1175/1520-0450(1984)023<0201:OTAVOC>2.0.CO;2. February 1984  
860

861 Wiles, G.C., Charlton, J., Wilson, R.J., D'Arrigo, R.D., Buma, B., Krapek, J., Gaglioti, B.V., Wiesenberg, N., Oelkers, R.:  
862 Yellow-cedar blue intensity tree-ring chronologies as records of climate in Juneau, Alaska, USA. *Canadian Journal of Forest*  
863 *Research* 49(12), 1483-1492. DOI: 10.1139/cjfr-2018-0525. September 2019  
864

865 Wilmking, M., van der Maaten-Theunissen, M., van der Maaten, E., Scharnweber, T., Buras, A., Biermann, C., Gurskaya,  
866 M., Hallinger, M., Lange, J., Shetti, R. and Smiljanic, M.: Global assessment of relationships between climate and tree  
867 growth. *Global Change Biology*, 26(6), pp.3212-3220. DOI: 10.1111/gcb.15057. March 2020  
868

869 Wilson, R.J. and Hopfmueller, M.: Dendrochronological investigations of Norway spruce along an elevational transect in the  
870 Bavarian Forest, Germany. *Dendrochronologia*, 19(1), pp.67-79. 2001  
871

872 Wilson, R.J. and Luckman, B.H.: Dendroclimatic reconstruction of maximum summer temperatures from upper treeline sites  
873 in Interior British Columbia, Canada. *The Holocene*, 13(6), pp.851-861. DOI: 10.1191/0959683603hl663rp. November 2003  
874

875 Wilson, R. and Elling, W.: Temporal instability in tree-growth/climate response in the Lower Bavarian Forest region:  
876 implications for dendroclimatic reconstruction. *Trees*, 18(1), pp.19-28. DOI: 10.1007/s00468-003-0273-z. January 2004.  
877

878 Wilson, R.J.S, Rao, R., Rydval, M., Wood, C., Larsson, L.-A., Luckman, B.H.: Blue Intensity for Dendroclimatology: The  
879 BC Blues: A Case Study from British Columbia Canada. *The Holocene* 24 (11), 1428-1438. DOI:  
880 10.1177/0959683614544051. August 2014  
881

882 Wilson, R., Wilson, D., Rydval, M., Crone, A., Büntgen, U., Clark, S., Ehmer, J., Forbes, E., Fuentes, M., Gunnarson, B.E.,  
883 Linderholm, H., Nicolussi, K., Wood, C., Mills, C.: Facilitating tree-ring dating of historic conifer timbers using Blue  
884 Intensity. *Journal of Archaeological Science* 78, 99-111. DOI: 10.1016/j.jas.2016.11.011. February 2017a  
885

886 Wilson, R., D'Arrigo, R., Andreu-Hayles, L., Oelkers, R., Wiles, G., Anchukaitis, K., Davi, N.: Experiments based on blue  
887 intensity for reconstructing North Pacific temperatures along the Gulf of Alaska. *Climate of the Past* 13(8), 1007-1022.  
888 doi.org/10.5194/cp-13-1007-2017. March 2017b  
889

890 Wilson, R., Anchukaitis, K., Andreu-Hayles, L., Cook, E., D'Arrigo, R., Davi, N., Haberbauer, L., Krusic, P., Luckman, B.,  
891 Morimoto, D., Oelkers, R., 2019. Improved dendroclimatic calibration using blue intensity in the southern Yukon. *The*  
892 *Holocene* 29(11), 1817-1830. DOI: 10.1177/0959683619862037. July 2019  
893  
894 Xiong, L., Okada, N., Fujiwara, T., Ohta, S. and Palmer, J.G.: Chronology development and climate response analysis of  
895 different New Zealand pink pine (*Halocarpus biformis*) tree-ring parameters. *Canadian Journal of Forest Research*, 28(4),  
896 pp.566-573. DOI: 10.1139/cjfr-28-4-566. April 1998  
897  
898 Yasue, K., Funada, R., Kobayashi, O. and Ohtani, J.: The effects of tracheid dimensions on variations in maximum density  
899 of *Picea glehnii* and relationships to climatic factors. *Trees*, 14(4), pp.223-229. DOI: 10.1007/PL00009766. February 2000  
900  
901 Young, G.H., Loader, N.J., McCarroll, D., Bale, R.J., Demmler, J.C., Miles, D., Nayling, N.T., Rinne, K.T., Robertson, I.,  
902 Watts, C. and Whitney, M.: Oxygen stable isotope ratios from British oak tree-rings provide a strong and consistent record  
903 of past changes in summer rainfall. *Climate Dynamics*, 45(11-12), pp.3609-3622. DOI: 10.1007/s00382-015-2559-4. March  
904 2015